Analysis of a Time Delay Controller Based on Convolutions - with Application to a Cruise Control System

by

Shih-Ying Huang

B.S., Mechanical Engineering (1988)

National Taiwan University

Submitted to the Department of Mechanical Engineering

in Partial Fulfillment of the Requirements for the degree of

Master of Science in Mechanical Engineering

at the

Massachusetts Institute of Technology

May, 1993

Signature of Author _____

Department of Mechanical Engineering
May 7, 1993

Certified by _____

Dr. Kamal Youcef-Toumi
Associate Professor
Thesis Supervisor

Accepted by _____

Dr. Ain A. Sonin
Chairman, Department Committee on Graduate Students

Analysis of a Time Delay Controller Based on Convolutions - with Application to a Cruise Control System

by

Shih-Ying Huang

Submitted to the Department of Mechanical Engineering
on May 7, 1993 in partial fulfillment of the
requirements for the degree of Master of Science in
Mechanical Engineering

ABSTRACT

Time Delay Control has been proposed as an effective control method for a class of systems with unknown dynamics and unpredictable disturbances. The control algorithm uses recent past data to estimate the uncertain dynamics and disturbances in the system. This Thesis presents a method based on convolutions to attenuate the noise amplification in the calculation of the estimated functions. This method suggests a delay time to be much larger than the sampling period. Through the accuracy analysis, an extrapolation scheme is found to be useful to improve the performance while keeping the delay time at an appropriate level. Stability analysis shows that a trade-off exists between robustness and performance. For a special class of systems with slow changing dynamics during the delay time, the convolution method with an extrapolation scheme is shown to provide a very satisfactory performance.

An application of Time Delay Control to an intelligent automotive cruise control system is presented to show the performance of Time Delay Controller on actual systems. In this system, a vehicle is equipped with a ranging sensor which measures the distance between a preceding car and itself. The relative distance between the two vehicles is the control output [the state] of the system and the dynamics of the leading car are treated as a disturbance. The performance of the Time Delay Control Method in this intelligent longitudinal cruise control system was evaluated using a one-fifth scale car model. Through simulations and experiments, the Time Delay Control technique is shown to be well suited for intelligent cruise controls because of its rapid estimation of system dynamics changes and ease of implementation. If noise is a significant problem, the method based on convolutions and extrapolations can be used to attenuate the noise while keeping a good performance. This implementation and the above analysis show that the flexibility and feasibility of Time Delay Controller are largely increased by the method based on convolutions.

Thesis Supervisor: Dr. Kamal Youcef-Toumi

Title: Associate Professor of Mechanical Engineering

Acknowledgement

I would like to express my deepest thanks to my advisor, Professor Kamal Youcef-Toumi. His valuable advice and continuous encouragement have helped me accomplish this work and learn knowledges beyond the books.

I would like to thank Shang Teh Wu for his valuable suggestions. The discussions with him always inspired me to try new ideas.

I appreciate my partner Yoshihiro Sasage for his help on the experiments and his lessons on the hardwares. It was a great pleasure to work with him.

I would like to thank my parents. It is their continuous encouragement and support allows me to focus my full concentration on my study at MIT.

Finally, I would like to thank Nippondenso Co. Ltd. for supporting this research.

Contents

List of Figures

Chapter 1
Introduction

1.1 Motivation of Thesis

The demand for high performance systems has introduced an increasingly challenging controller design problem. These systems include machines with significant dynamic changes operating in environments where unpredictable disturbances are possible. To guarantee high performance, a fast adaptation control method which can deal with unknown dynamics and unpredictable disturbances is necessary.

Several types of control strategies have been developed to deal with this problem. In Adaptive Control [1,6,7,11] the structure of the controller is selected a priori, usually PD or PID. The controller gains are then updated using recursively estimated parameters of the plant. As stated in [3,4], this method considers slowly varying parameters, linear dynamic equations, and/or bounded uncertainty. This technique is therefore unacceptable for some applications that need high adaptation rates. One example is the control of magnetic bearings. In order to guarantee stability and appropriate disturbance rejection properties, the controller must detect disturbances within 200 μsec [22]. Sliding mode control [8,13,14] can accommodate nonlinear systems. Based on Lyapunov's method, the control scheme is characterized by discontinuous function with high frequency chattering. Sliding mode control action involves a term depending on the system model. Therefore, if uncertainty is small, the error is small. However, when systems has potentially significant uncertainties, the per-

formance would not be acceptable. Learning control [2,5,12] is an approach which is based on trial and error. Each time the system performs the same task, data is collected and used to update the control action. By repeating the task several times, performance can be improved. This approach is well suited to repetitive tasks and may not be appropriate for other types of systems. Control algorithms based on table look up, such as gain adjustment control, have been used extensively in automotive applications for engine control and anti-skid braking systems. To implement this control and obtain good performance, a significant amount of experimental data needs to be taken and stored in the controller. The stored data must also be specific for each different type of machine. A degradation of performance will occur as mechanical components wear. For some high performance systems which need fast adaption rates to cope with significant and fast changing dynamics and disturbances, the current methods mentioned above might have some problems when implementing in one way or another.

Time Delay Control [15,16,17,18,19] has been proposed to be a method that can deal with this problem for a class of systems. Time Delay Control depends on neither estimation of specific parameters, discontinuous control, nor repetitive actions. Rather, it depends on the direct estimation of a function representing the effect of uncertainties. This is accomplished using time delay. The gathered information is used to cancel the unknown dynamics and the unexpected disturbances simultaneously. Then the controller inserts the desired dynamics into the plant. In other words, the Time Delay Controller uses past observation of the system's response and the control input to directly modify the control actions rather than adjusting the controller gains or identifying the system parameters, thereby leading to a model independent and fast adaption controller. This algorithm can deal with large unpredictable system

parameter variations and disturbances. Yet the system's performance is very satisfactory. The successful implementations include : servosystems, robot manipulators and high speed active magnetic bearing systems for rotors.

However, using the original form of Time Delay Controller, a digital differentiation inevitably amplifies the noise. For some applications, the performances become unacceptable. Therefore, it is necessary to modify Time Delay Controllers to reduce this amplification.

1.2 Contents of Thesis

In this thesis, a class of time delay controllers using convolutions to evaluate the net disturbance consisting of unknown system dynamics and unexpected disturbances are presented. This method suggests a calculation using the data in a small moving observation window to reduce the noise amplification caused by the digital differentiation in the original method. Based on this evaluation, an extrapolation method is proposed to improve the performance. The accuracy of evaluation and the stability conditions of these controllers are also discussed. An application to a cruise control system is used to demonstrate the performance of TDC on actual systems. This thesis is organized as follows. Chapter 2 derives the convolution type of Time Delay Control law. Chapter 3 discusses the accuracy of the evaluation based on the convolution methods. Chapter 4 gives the stability conditions of these time delay controllers. Chapter 5 studies the frequency response of controllers based on convolutions and extrapolations. Chapter 6 presents an example by a two degree of freedom robot manipulator. Chapter 7 presents an experiment on an intelligent cruise control system. The conclusions are summarized in Chapter 8.

Chapter 2

A Control Law Based on Convolutions

2.1 System Description

The systems under considerations are described as

$$\dot{\mathbf{x}} = \mathbf{F}(\mathbf{x}, t) + \mathbf{H}(\mathbf{x}, t) + \mathbf{B}(\mathbf{x})\mathbf{u} + \mathbf{D}(t) \tag{2.1}$$

where $\mathbf{x} \in \Re^n$ is the plant state vector and $\mathbf{u} \in \Re^r$ is a control vector. $\mathbf{F}(\mathbf{x}, t)$ and $\mathbf{H}(\mathbf{x}, t) \in \Re^n$ are nonlinear vectors representing respectively the known and unknown part of the plant dynamics, and $\mathbf{D}(t) \in \Re^n$ is an unknown disturbance vector. The variable t represents time. In this paper we are concerned with the class of systems satisfy a matching condition described in [25]. These systems can be partitioned as

$$\mathbf{x}(t) = \begin{bmatrix} \mathbf{x}_q(t) \\ ... \\ \mathbf{x}_r(t) \end{bmatrix}; \quad \mathbf{F}(\mathbf{x}, t) = \begin{bmatrix} \mathbf{x}_s(t) \\ ... \\ \mathbf{F}_r(\mathbf{x}, t) \end{bmatrix}; \quad \mathbf{H}(\mathbf{x}, t) = \begin{bmatrix} 0 \\ ... \\ \mathbf{H}_r(\mathbf{x}, t) \end{bmatrix} \tag{2.2}$$

$$\mathbf{D}(t) = \begin{bmatrix} 0 \\ ... \\ \mathbf{D}_r(t) \end{bmatrix}; \quad \mathbf{B}(\mathbf{x}) = \begin{bmatrix} 0 \\ ... \\ \mathbf{B}_r(\mathbf{x}) \end{bmatrix} \tag{2.3}$$

where the partial states are $\mathbf{x}_q(t) \in \Re^{n-r}$, $\mathbf{x}_r(t) \in \Re^r$, $\mathbf{x}_s(t) = [\mathbf{x}_{r+1}, \mathbf{x}_{r+1}, ..., \mathbf{x}_n]^T \in \Re^{n-r}$. The vector functions are $\mathbf{F}_r(\mathbf{x}, t) \in \Re^r$, $\mathbf{H}_r(\mathbf{x}, t) \in \Re^r$ and $\mathbf{B}_r(\mathbf{x}) \in \Re^{r \times r}$. A reference model that generates the desired trajectory is chosen as a linear time invariant system,

$$\dot{\mathbf{x}}_m = \mathbf{A}_m \mathbf{x}_m + \mathbf{B}_m r \tag{2.4}$$

The matrices are also partitioned in the same manner

$$\mathbf{A}_m = \begin{bmatrix} 0 & | & \mathbf{I}_{n-r} \\ & ... & \\ & \mathbf{A}_{mr} & \end{bmatrix}; \quad \mathbf{B}_m = \begin{bmatrix} 0 \\ ... \\ \mathbf{B}_{mr} \end{bmatrix} \tag{2.5}$$

where $\mathbf{I}_{n-r} \in \Re^{n-r \times n-r}$, $\mathbf{A}_{mr} \in \Re^{r \times n}$, $\mathbf{B}_{mr} \in \Re^{r \times r}$,$\mathbf{B}_m \in \Re^{n \times r}$ and $\mathbf{r}(t) \in \Re^r$. To transform Eqn(2.1) to a general form with a known constant control distribution matrix, we rewrite Eqn(2.1) as

$$\dot{\mathbf{x}} = \mathbf{F}(\mathbf{x}, t) + \mathbf{\Psi}(\mathbf{x}, \mathbf{u}, t) + \hat{\mathbf{B}}\mathbf{u} \tag{2.6}$$

where the unknown function $\mathbf{\Psi}(\mathbf{x}, \mathbf{u}, t)$ is defined as

$$\mathbf{\Psi}(\mathbf{x}, \mathbf{u}, t) = \begin{bmatrix} 0 \\ ... \\ \mathbf{\Psi}_r(\mathbf{x}, \mathbf{u}, t) \end{bmatrix} = \mathbf{H}(\mathbf{x}, t) + \mathbf{D}(t) + [\mathbf{B}(\mathbf{x}) - \hat{\mathbf{B}}]\mathbf{u} \tag{2.7}$$

and $\hat{\mathbf{B}}$ in the form of

$$\hat{\mathbf{B}} = \begin{bmatrix} 0 \\ ... \\ \hat{\mathbf{B}}_r \end{bmatrix} \tag{2.8}$$

is a constant matrix of rank r to be selected by the designer.

2.2 Derivation of Control Law

The purpose of control is to force the states of the system to follow the state trajectories of the reference model. Thus the error vector $\mathbf{e} \in \Re^n$ is defined as

$$\mathbf{e} = \mathbf{x}_m - \mathbf{x} \tag{2.9}$$

The time rate of change of the error, $\dot{\mathbf{e}}$ is then

$$\dot{\mathbf{e}} = \dot{\mathbf{x}}_m - \dot{\mathbf{x}} \tag{2.10}$$

Combining Eqn(2.6) and Eqn(2.4), one can obtain

$$\dot{\mathbf{e}} = \mathbf{A}_m\mathbf{x}_m + \mathbf{B}_m r - [\mathbf{F}(\mathbf{x}, t) + \mathbf{\Psi}(\mathbf{x}, \mathbf{u}, t) + \hat{\mathbf{B}}\mathbf{u}] \tag{2.11}$$

To bring about an error term, the term $\mathbf{A}_m\mathbf{x}$ can be added and subtracted to the above equation, which leads to

$$\dot{\mathbf{e}} = \mathbf{A}_m\mathbf{x}_m + \mathbf{B}_m\mathbf{r} - [\mathbf{F}(\mathbf{x},t) + \mathbf{\Psi}(\mathbf{x},\mathbf{u},t) + \hat{\mathbf{B}}\mathbf{u}] + \mathbf{A}_m\mathbf{x} - \mathbf{A}_m\mathbf{x} \tag{2.12}$$

and then Eqn(2.12) can be rewritten as

$$\dot{\mathbf{e}} = \mathbf{A}_m\mathbf{e} + [\mathbf{A}_m\mathbf{x} + \mathbf{B}_m\mathbf{r} - \mathbf{F}(\mathbf{x},t) - \mathbf{\Psi}(\mathbf{x},\mathbf{u},t) - \hat{\mathbf{B}}\mathbf{u}] \tag{2.13}$$

Now a control action $\mathbf{u}$ can be chosen such that the term between brackets in Eqn.(2.13) is zero at any instant of time. This makes the error decay at the rate dictated by the reference system model $\mathbf{A}_m$. Since this decay rate is not practical in general, a much faster one is desired. So a new control action

$$\mathbf{v} = \mathbf{u} + \mathbf{K}\mathbf{e} \tag{2.14}$$

is defined to adjust the error dynamics, where $\mathbf{K} \in \Re^{r\times n}$ is a feedback gain matrix. The error dynamics now takes the form

$$\dot{\mathbf{e}} = [\mathbf{A}_m + \hat{\mathbf{B}}\mathbf{K}]\mathbf{e} + \mathbf{p} \tag{2.15}$$

where $\mathbf{p}$ vector is

$$\mathbf{p} = \mathbf{A}_m\mathbf{x} + \mathbf{B}_m\mathbf{r} - \mathbf{F}(\mathbf{x},t) - \mathbf{\Psi}(\mathbf{x},\mathbf{u},t) - \hat{\mathbf{B}}\mathbf{v} \tag{2.16}$$

The control law is chosen as

$$\mathbf{v} = \hat{\mathbf{B}}^{+}[\mathbf{A}_m\mathbf{x} + \mathbf{B}_m\mathbf{r} - \mathbf{F}(\mathbf{x},t) - \mathbf{\Psi}(\mathbf{x},\mathbf{u},t)] \tag{2.17}$$

where $\hat{\mathbf{B}}^{+} \in \Re^{r\times n}$ is the pseudo-inverse matrix of $\hat{\mathbf{B}}$ defined as $(\hat{\mathbf{B}}^T\hat{\mathbf{B}})^{-1}\hat{\mathbf{B}}^T$. For the form of Eqn(2.8), $\hat{\mathbf{B}}^{+}$ is given by

$$\hat{\mathbf{B}}^{+} = [0 \mid \hat{\mathbf{B}}_r^{-1}] \tag{2.18}$$

and the control law becomes

$$\mathbf{v} = \hat{\mathbf{B}}_r^{-1}[\mathbf{A}_{mr}\mathbf{x} + \mathbf{B}_{mr}\mathbf{r} - \mathbf{F}_r(\mathbf{x},t) - \mathbf{\Psi}_r(\mathbf{x},\mathbf{u},t)] \tag{2.19}$$

The dynamic behavior of the error is governed by Eqn.(2.15) and its time response

$$\mathbf{e}(t) = \mathbf{e}^{(\mathbf{A}_m+\hat{\mathbf{B}}\mathbf{K})(t-t_0)}\mathbf{e}(t_0) + \int_{t_0}^{t} e^{(\mathbf{A}_m+\hat{\mathbf{B}}\mathbf{K}))(t-\tau)}\mathbf{p}(\tau)d\tau \quad \forall t \geq t_0 \tag{2.20}$$

involves a state transition matrix $\mathbf{\Phi}(t,t_0)$,

$$\mathbf{\Phi}(t,t_0) = e^{(\mathbf{A}_m+\hat{\mathbf{B}}\mathbf{K})(t-t_0)} = e^{\mathbf{A}_e(t-t_0)} \quad \forall t \geq t_0 \tag{2.21}$$

If $\mathbf{A}_m$, $\hat{\mathbf{B}}$, and $\mathbf{K}$ are specified along with $\mathbf{e}(t_0)$, the unknown function can be estimated through rearranging Eqn.(2.20) by

$$\begin{aligned}\int_{t_0}^{t} \mathbf{\Phi}(t,\tau)\mathbf{\Psi}(\tau)d\tau &= -\mathbf{e}(t) + \mathbf{\Phi}(t,t_0)\mathbf{e}(t_0) + \int_{t_0}^{t} \mathbf{\Phi}(t,\tau)\mathbf{A}_m\mathbf{x}(\tau)d\tau \\ &\quad + \int_{t_0}^{t} \mathbf{\Phi}(t,\tau)\mathbf{B}_m\mathbf{r}(\tau)d\tau - \int_{t_0}^{t} \mathbf{\Phi}(t,\tau)\mathbf{F}(\tau)d\tau \\ &\quad - \int_{t_0}^{t} \mathbf{\Phi}(t,\tau)\hat{\mathbf{B}}\mathbf{v}(\tau)d\tau \end{aligned} \tag{2.22}$$

If $\mathbf{\Psi}(t)$ doesn't change significantly during the interval $[t_0,t]$, we can approximate it as $\hat{\mathbf{\Psi}}(t)$ by the following Equation

$$\left[\int_{t_0}^{t} \mathbf{\Phi}(t,\tau)d\tau\right]\hat{\mathbf{\Psi}}(t) = \int_{t_0}^{t} \mathbf{\Phi}(t,\tau)\mathbf{\Psi}(\tau)d\tau \tag{2.23}$$

and thus

$$\hat{\mathbf{\Psi}}(t) = \left[\int_{t_0}^{t} \mathbf{\Phi}(t,\tau)d\tau\right]^{-1}\left[\int_{t_0}^{t} \mathbf{\Phi}(t,\tau)\mathbf{\Psi}(\tau)d\tau\right] \tag{2.24}$$

Once the unknown function is obtained, the control action can be calculated by Eqn (2.19). This control law, when implemented digitally, suggests a delay time L to be much larger than the sampling period t_s as shown in Fig(2.1). One of the benefits

in doing this is to attenuate the high frequency noise effects. However, there are at least two other problems we should investigate about this control law. One is the accuracy of the approximation of $\mathbf{\Psi}$ by $\hat{\mathbf{\Psi}}$. This accuracy, as one can understand by intuition, depends on the window size and determines the performance of the whole system. Another issue is the stability conditions of the closed loop system under the assumption that the window size is sufficiently small. This condition, as what will be shown in the following chapters, involves the matrices $\hat{\mathbf{B}}$, $\mathbf{B}(\mathbf{x})$ and the state transition matrix $\mathbf{\Phi}$.

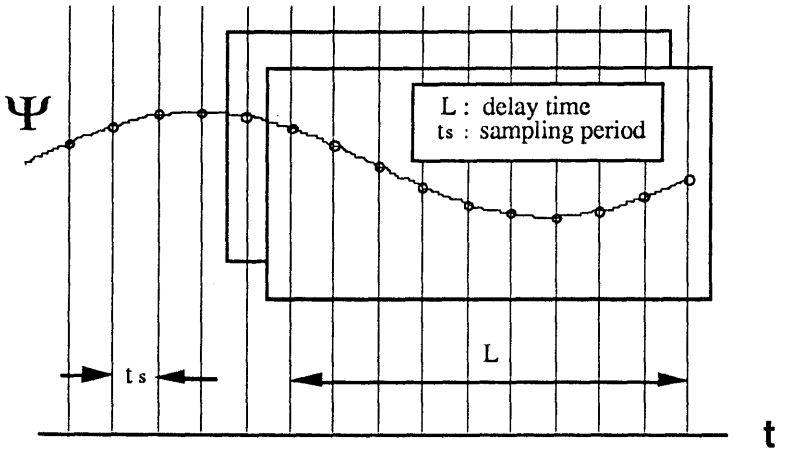

Figure 2.1: A Moving Observation Window

2.3 Digital Implementation

By examining Eqn (2.19), Eqn (2.22) and Eqn (2.24), one can find out that there exists a causal conflict and therefore an algebraic loop forms. The reason is that in Eqn (2.19), $\mathbf{v}(t)$ depends on $\mathbf{\Phi}(t)$ and in Eqn (2.22), $\mathbf{\Phi}(t)$ depends on the integral $\int_{t_0}^{t} \mathbf{\Phi}(t,\tau)\hat{\mathbf{B}}\mathbf{v}(\tau)d\tau$. To avoid this problem, the integral $\int_{t_0}^{t} \mathbf{\Phi}(t,\tau)\hat{\mathbf{B}}\mathbf{v}(\tau)d\tau$ has to be replaced by a delayed integral $\int_{t_0-\Delta t}^{t-\Delta t} \mathbf{\Phi}(t,\tau)\hat{\mathbf{B}}\mathbf{v}(\tau)d\tau$, where Δt is a small time period.

However, if a digital controller is used to implement this control law, the inherent time delay caused by digital sampling solves this problem automatically, and the algebraic loop will no longer exist. In this case, the equations (2.19), (2.22) and (2.24) are approximated as

$$\mathbf{v}_{(k)} = \hat{\mathbf{B}}^{-1}[\mathbf{A}_m\mathbf{x}_{(k)} + \mathbf{B}_m\mathbf{r}_{(k)} - \mathbf{F}_{(k)} - \hat{\mathbf{\Psi}}_{(k)}] \tag{2.25}$$

$$\hat{\mathbf{\Psi}}_{(k)} = \left[\sum_{n=0}^{q-1} e^{\mathbf{A}_e(q-n)t_s}t_s\right]^{-1}\left[\sum_{n=0}^{q-1} e^{\mathbf{A}_e(q-n)t_s}\mathbf{\Psi}_{(k-(q-n))}t_s\right] \tag{2.26}$$

$$\begin{aligned}\sum_{n=0}^{q-1} e^{\mathbf{A}_e(q-n)t_s}\mathbf{\Psi}_{(k-(q-n))}t_s \;\simeq\; & -\mathbf{e}_{(k)} + e^{\mathbf{A}_e q t_s}\mathbf{e}_{(k-q)} + \sum_{n=0}^{q-1} e^{\mathbf{A}_e(q-n)t_s}[\mathbf{A}_m\mathbf{x}_{(k-(q-n))} \\ & +\mathbf{B}_m\mathbf{r}_{(k-(q-n))} - \mathbf{F}_{(k-(q-n))} - \hat{\mathbf{B}}\mathbf{v}_{(k-(q-n))}]t_s\end{aligned} \tag{2.27}$$

where k represents the digital step, t_s is the sampling period, q is the number of data points in the moving window, and thus $t - t_0 = qt_s$.

2.4 An Equivalent Form

Eqn(2.22) can be written in a different form. Using this form, as what will be shown, when $\mathbf{K}$ is chosen as $\mathbf{0}$, i.e. $\mathbf{A}_e = \mathbf{A}_m$, the signal $\mathbf{e}$ is not included in the evaluation of the unknown function, therefore the calculation of $\mathbf{x}_m(t)$ is not necessary.

Since Eqn(2.4) can be written in the form,

$$\begin{aligned}\dot{\mathbf{x}}_m &= \mathbf{A}_m\mathbf{x}_m + \mathbf{B}_m\mathbf{r} \\ &= (\mathbf{A}_m + \hat{\mathbf{B}}\mathbf{K})\mathbf{x}_m + \mathbf{B}_m\mathbf{r} - \hat{\mathbf{B}}\mathbf{K}\mathbf{x}_m\end{aligned} \tag{2.28}$$

the following equation is obtained.

$$\mathbf{x}_m(t) = \mathbf{\Phi}(t,t_0)\mathbf{x}_m(t_0) + \int_{t_0}^{t}\mathbf{\Phi}(t,\tau)\mathbf{B}_m\mathbf{r}(\tau)d\tau - \int_{t_0}^{t}\mathbf{\Phi}(t,\tau)\mathbf{B}\mathbf{K}\mathbf{x}_m(\tau)d\tau \tag{2.29}$$

The simplification form of Eqn(2.22) then is

$$\begin{aligned}\int_{t_0}^{t} \mathbf{\Phi}(t,\tau)\mathbf{\Psi}(\tau)d\tau &= \mathbf{x}(t) - \mathbf{\Phi}(t,t_0)\mathbf{x}(t_0) \\ &\quad + \int_{t_0}^{t} \mathbf{\Phi}(t,\tau)(\mathbf{A}_m + \hat{\mathbf{B}}\mathbf{K})\mathbf{x}(\tau)d\tau - \int_{t_0}^{t} \mathbf{\Phi}(t,\tau)\mathbf{F}(\tau)d\tau \\ &\quad - \int_{t_0}^{t} \mathbf{\Phi}(t,\tau)\hat{\mathbf{B}}\mathbf{u}(\tau)d\tau \qquad (2.30)\end{aligned}$$

The corresponding digital form can be obtained by approximating the integrations by summations.

$$\begin{aligned}\sum_{n=0}^{q-1} e^{\mathbf{A}_e(q-n)t_s}\mathbf{\Psi}_{(k-(q-n))}t_s &\simeq \mathbf{x}_{(k)} - e^{\mathbf{A}_e q t_s}\mathbf{x}_{(k-q)} + \sum_{n=0}^{q-1} e^{\mathbf{A}_e(q-n)t_s}[\mathbf{A}_e\mathbf{x}_{(k-(q-n))} \\ &\quad -\mathbf{F}_{(k-(q-n))} - \hat{\mathbf{B}}\mathbf{u}_{(k-(q-n))}]t_s \qquad (2.31)\end{aligned}$$

In this form, only $\mathbf{x}$ and $\mathbf{u}$ is used to evaluate the unknown function. If $\mathbf{K}$ is chosen as $\mathbf{0}$, then $\mathbf{v} = \mathbf{u}$ is used as the control input, that is, no calculations of $\mathbf{x}_m(t)$ is necessary.

2.5 Special Cases

The control law derived above is a general form of Time Delay Controller based on convolutions. Under some conditions, the control law can be reduced to simpler forms. Those simpler forms of control law can be derived by other approaches, but in fact they are special cases of the derived control law.

2.5.1 The Original Form of TDC

When only one past data point is used in the evaluation of the unknown function, Eqn (2.26) and (2.31) lead to

$$\begin{aligned}\hat{\mathbf{\Psi}}_{(k)} &= \left[e^{\mathbf{A}_e t_s}t_s\right]^{-1}\left[e^{\mathbf{A}_e t_s}\mathbf{\Psi}_{(k-1)}t_s\right] \\ &\simeq \left[e^{\mathbf{A}_e t_s}t_s\right]^{-1}\mathbf{x}_{(k)} - \frac{1}{t_s}\mathbf{x}_{(k-1)} + \left[\mathbf{A}_m\mathbf{x}_{(k-1)} - \mathbf{F}_{(k-1)} - \hat{\mathbf{B}}\mathbf{v}_{(k-1)}\right] \qquad (2.32)\end{aligned}$$

Note that

$$\mathbf{e}_{(k)} = \mathbf{x}_{m(k)} - \mathbf{x}_{(k)} \tag{2.33}$$

and

$$\mathbf{v}_{(k)} = \mathbf{u}_{(k)} + \mathbf{K}\mathbf{e}_{(k)} \tag{2.34}$$

Through some calculations [1], the following result is obtained.

$$\hat{\mathbf{\Psi}}_{(k)} = \frac{1}{t_s}\left[\mathbf{x}_{(k)} - \mathbf{x}_{(k-1)}\right] - \mathbf{F}_{(k-1)} - \hat{\mathbf{B}}\mathbf{u}_{(k-1)} \tag{2.35}$$

Eqn (2.35) is the evaluation used in the original form of TDC, where $\frac{1}{t_s}\left[\mathbf{x}_{(k)} - \mathbf{x}_{(k-1)}\right]$ is a digital differentiation of $\mathbf{x}(t)$. If the signal $\mathbf{x}(t)$ is noisy, $\frac{1}{t_s}$ will produce significant amplification, and the performance will not be acceptable.

2.5.2 TDC Based on Integrations without Weighting Factors

In Eqn (2.26), $\hat{\mathbf{\Psi}}(t)$ can be interpreted as the weighting average of the unknown function $\mathbf{\Psi}(t)$ through a period $[t_0, t]$. If the weighting factors are ignored, Eqn (2.31) becomes

$$\hat{\mathbf{\Psi}}_{(k)} = \frac{1}{L}\left[\mathbf{x}_{(k)} - \mathbf{x}_{(k-q)}\right] + \frac{1}{L}\sum_{n=0}^{q-1}\left[-\mathbf{F}_{(k-(q-n))} - \hat{\mathbf{B}}\mathbf{u}_{(k-(q-n))}\right] \tag{2.36}$$

where $L = qt_s$ is the delay time $t - t_0$. This form can be also obtained by integrating Eqn (2.6) and approximating the integrations by summations.

2.6 Numerical Example

A simple second order system was chosen to perform some numerical calculations,

$$\dot{\mathbf{x}} = \frac{d}{dt}\begin{bmatrix} x_1 \\ x_2 \end{bmatrix} = \begin{bmatrix} x_2 \\ 0.1x_2^2 \end{bmatrix} + \begin{bmatrix} 0 \\ b \end{bmatrix} u + \begin{bmatrix} 0 \\ d(t) \end{bmatrix} \tag{2.37}$$

[1] A necessary approximation $e^{\mathbf{A}_e t_s} \simeq \mathbf{I} + \mathbf{A}_e t_s$ has to be made.

where $d(t)$ is an unknown disturbance. The reference model is chosen as a second order system with a damping ratio $\xi = 1$ and a natural frequency $\omega_n = 5\ rad/sec.$ The reference input is a unit step . Thus the reference model is

$$\dot{\mathbf{x}}_m = \frac{d}{dt}\begin{bmatrix} x_{m1} \\ x_{m2} \end{bmatrix} = \begin{bmatrix} 0 & 1 \\ -25 & -10 \end{bmatrix}\begin{bmatrix} x_{m1} \\ x_{m2} \end{bmatrix} + \begin{bmatrix} 0 \\ 25 \end{bmatrix} r \tag{2.38}$$

The unknown function $\mathbf{\Psi}_r$ in this example is

$$\psi_2 = 0.1(x_2)^2 + d(t) + (25 - \hat{b})u \tag{2.39}$$

If the delay time is 0.01 *sec*, and the sampling period is 0.005 *sec*, the control action according to Eqn (2.19) and Eqn (2.24) is then

$$u_{(k)} = \hat{b}^{-1}[-25x_{1(k)} - 10x_{2(k)} + 25r_{(k)} - \hat{\psi}_{2(k)}] \tag{2.40}$$

where

$$\begin{aligned} \hat{\psi}_{2(k)} = {} & 19.38e_{1(k)} - 107.69e_{2(k)} - 6.25e_{1(k-2)} + 97.50e_{2(k-2)} \\ & -12.81x_{1(k-1)} - 5.09x_{2(k-1)} + 12.81r_{(k-1)} - 0.51\hat{b}u_{(k-1)} \\ & -12.19x_{1(k-2)} - 4.91x_{2(k-2)} + 12.19r_{(k-2)} - 0.49\hat{b}u_{(k-2)} \end{aligned} \tag{2.41}$$

Note that usually more points are used to evaluate the unknown function so that the control action is nearly continuous and therefore the system response is also smooth.

Chapter 3

Analysis of Accuracy

3.1 Analysis of Accuracy for Continuous Systems

To examine the accuracy of the approximation of Eqn(2.23), Taylor's expansion is used to express the estimation error. First, if a vector function $\mathbf{f}(t)$ is analytic for all $t > 0$ and $\mathbf{f}(t) = 0$ for all $t < 0$, $\mathbf{f}(t-L)$ can be expanded around t for all $t > L$,

$$\mathbf{f}(t-L) = \mathbf{f}(t) - \mathbf{f}'(t)L + \frac{\mathbf{f}''(t)L^2}{2!} - \frac{\mathbf{f}'''(t)L^3}{3!} + ... \tag{3.1}$$

Taking the integral of both sides and rearranging the equation, the following form is obtained.

$$\mathbf{f}(t) = \frac{1}{L}\int_0^t [\mathbf{f}(\tau) - \mathbf{f}(\tau - L)]d\tau + \frac{\mathbf{f}'(t)L}{2!} - \frac{\mathbf{f}''(t)L^2}{3!} + ... \tag{3.2}$$

Since

$$\int_0^t \mathbf{f}(\tau - L)d\tau = \int_{-L}^{t-L} \mathbf{f}(s)ds = \int_0^{t-L} \mathbf{f}(s)ds \tag{3.3}$$

if $\tau - L$ is taken as s. Eqn(3.2) can be written as

$$\mathbf{f}(t) = \frac{1}{L}\int_{t-L}^t \mathbf{f}(\tau)d\tau + \frac{\mathbf{f}'(t)L}{2!} - \frac{\mathbf{f}''(t)L^2}{3!} + ... \tag{3.4}$$

Assume $\mathbf{\Psi}(t)$ is analytic for all $t > 0$, let $\mathbf{f}(t) = e^{-\mathbf{A}_e t}\mathbf{\Psi}(t)$ and substitute into Eqn(2.24).

$$e^{-\mathbf{A}_e t}\mathbf{\Psi}(t) = \frac{1}{L}\int_{t-L}^t e^{-\mathbf{A}_e \tau}\mathbf{\Psi}(\tau)d\tau + \frac{[e^{-\mathbf{A}_e t}\mathbf{\Psi}(t)]'(t)L}{2!} - \frac{[e^{-\mathbf{A}_e t}\mathbf{\Psi}(t)]''(t)L^2}{3!} + ...(3.5)$$

Calculating the differentiations and rearranging the equation, the following equation is obtained

$$\mathbf{\Psi}(t) = \left[\int_{t-L}^{t} e^{\mathbf{A}_e(t-\tau)}d\tau\right]^{-1}\left[\int_{t-L}^{t} e^{\mathbf{A}_e(t-\tau)}\mathbf{\Psi}(\tau)d\tau + \frac{\mathbf{\Psi}'(t)}{2!}L - \frac{\mathbf{\Psi}''(t) - 2(\mathbf{A}_e)\mathbf{\Psi}'}{3!}L^2 + ...\right] \tag{3.6}$$

Note that the first term is the function which is used to evaluate the unknown function, and the other terms combine to represent the error of this evaluation. If the Fourier transform of the signal $\mathbf{\Psi}(t)$ is taken, and is denoted as $\mathcal{F}\{\mathbf{\Psi}\}(\omega)$, the signal $\mathbf{\Psi}(t)$ can be considered as the combination of infinite sinusoidal signals with frequency ω from $-\infty$ to ∞

$$\mathbf{\Psi}(t) = \frac{1}{2\pi}\int_{-\infty}^{\infty} \mathcal{F}\{\mathbf{\Psi}\}(\omega)e^{j\omega t}d\omega \tag{3.7}$$

Since Eqn(3.6) is linear, if the evaluation by a scalar sinusoidal unknown function with frequency ω is examined , it is found that when the dimensionless value ωL is small, the value of the right side terms in Eqn(3.6) is descending term by term. In this case, the evaluation is reasonable, and the order of accuracy is $\mathcal{O}(\omega L)$. When ωL is large or even greater than 1, this evaluation is very inaccurate. This shows that the evaluation of Eqn(2.24) can only evaluate the components in the signal $\mathbf{\Psi}(t)$ with frequency low enough to make ωL small.

When a digital controller is used, although the continuous equation (3.6) is no longer valid, if the sampling time is small enough, it still serves as a good approximation.

3.2 Extrapolation Methods based on Taylor's Expansion

Since the evaluation of unknown function is a numerical calculation, numerical analysis methods can be used to obtain a more accurate result. According to Eqn(3.6),

an extrapolation similar to Aitken's method [10] can be suggested to improve the performance. The evaluation is revised as

$$\hat{\mathbf{\Psi}}_{order2}(t) = 2T(\frac{L}{2}) - T(L) \tag{3.8}$$

$$= \mathbf{\Psi}(t) + \mathcal{O}(L)^2 \tag{3.9}$$

where

$$T(L) = [\int_{t-L}^{t} e^{\mathbf{A}_e(t-\tau)}d\tau]^{-1} \int_{t-L}^{t} e^{\mathbf{A}_e(t-\tau)}\mathbf{\Psi}(\tau)d\tau \tag{3.10}$$

or a more accurate evaluation

$$\hat{\mathbf{\Psi}}_{order3}(t) = \frac{8}{3}T(\frac{L}{4}) - 2T(\frac{L}{2}) + \frac{1}{3}T(L) \tag{3.11}$$

$$= \mathbf{\Psi}(t) + \mathcal{O}(L)^3 \tag{3.12}$$

The same procedure can be taken so that the error is reduced to be higher order of L, and the evaluation can be very accurate. If L is chosen as reasonably small, this method can improve the tracking error and reduce the settling time. But this method can only increase the accuracy of evaluation for the components in $\mathbf{\Psi}(t)$ with relatively low frequencies. The following sections show the simulation performance for an example, which has an unknown function with low changing rate. The result is then very satisfactory. However, compare to the unrevised evaluation, as we will show, the range of choosing $\hat{\mathbf{B}}$ is reduced, that is, the stability condition is more strict. This is a reasonable tread-off, since a larger stable region doesn't guarantee a good performance. This method at least suggests that when the knowledge about $\mathbf{B}(\mathbf{x})$ is good enough, extrapolation methods can be used to improve the controller.

3.3 Extrapolation Methods for Digital Systems

The digital forms of Eqn (3.8), (3.11) are obtained by approximating the integrals as summations.

$$\begin{aligned}\hat{\Psi}_{order2(k)} &= 2\left[\sum_{n=0}^{\frac{q}{2}-1} e^{\mathbf{A}_e(\frac{q}{2}-n)t_s}t_s\right]^{-1}\left[\sum_{n=0}^{\frac{q}{2}-1} e^{\mathbf{A}_e(\frac{q}{2}-n)t_s}\Psi_{(k-(\frac{q}{2}-n))}t_s\right] \\ &\quad -\left[\sum_{n=0}^{q-1} e^{\mathbf{A}_e(q-n)t_s}t_s\right]^{-1}\left[\sum_{n=0}^{q-1} e^{\mathbf{A}_e(q-n)t_s}\Psi_{(k-(q-n))}t_s\right] \qquad (3.13)\end{aligned}$$

$$\begin{aligned}\hat{\Psi}_{order3(k)} &= \frac{8}{3}\left[\sum_{n=0}^{\frac{q}{4}-1} e^{\mathbf{A}_e(\frac{q}{4}-n)t_s}t_s\right]^{-1}\left[\sum_{n=0}^{\frac{q}{4}-1} e^{\mathbf{A}_e(\frac{q}{4}-n)t_s}\Psi_{(k-(\frac{q}{4}-n))}t_s\right] \\ &\quad -2\left[\sum_{n=0}^{\frac{q}{2}-1} e^{\mathbf{A}_e(\frac{q}{2}-n)t_s}t_s\right]^{-1}\left[\sum_{n=0}^{\frac{q}{2}-1} e^{\mathbf{A}_e(\frac{q}{2}-n)t_s}\Psi_{(k-(\frac{q}{2}-n))}t_s\right] \\ &\quad +\frac{1}{3}\left[\sum_{n=0}^{q-1} e^{\mathbf{A}_e(q-n)t_s}t_s\right]^{-1}\left[\sum_{n=0}^{q-1} e^{\mathbf{A}_e(q-n)t_s}\Psi_{(k-(q-n))}t_s\right] \qquad (3.14)\end{aligned}$$

One thing worthy of noting is that, in this case, t_s should be chosen as about the same order of $(L)^2$ in Eqn(3.8) or $(L)^3$ in Eqn(3.11) so that the order of accuracy is consistent.

3.4 Example

A simple second order system as shown in section 2.6 Eqn (2.37) was chosen to show the performance of the controllers we mentioned above. In this example, d(t) is chosen as, for case I, a step disturbance with amplitude 1, and for case II, a sinusoidal signal with frequency 10 rad/sec and amplitude 1. The value b is assume to be known exactly. We choose the reference model as a second order system with $\xi = 1$ and $\omega_n = 5$ rad/sec and unit step reference input. The delay time is 0.1 sec, and the sampling period is 0.0025 sec. Fig(3.1) to Fig(3.6) show the results. Line 1,

2, 3 shows the simulation curve using Eqn(2.24), (3.8) and (3.11) respectively by a same window size L. From the results, we can see that while choosing a larger window to reduce the noise, we can use a more accurate evaluation of the unknown function to improve the performance. Although at the same time, because of the weighting in extrapolating calculation, the noise can be amplified, the scale of this amplification is much smaller than if we choose a small L to achieve the same performance. Fig(3.7) shows the control actions with noise in each case.

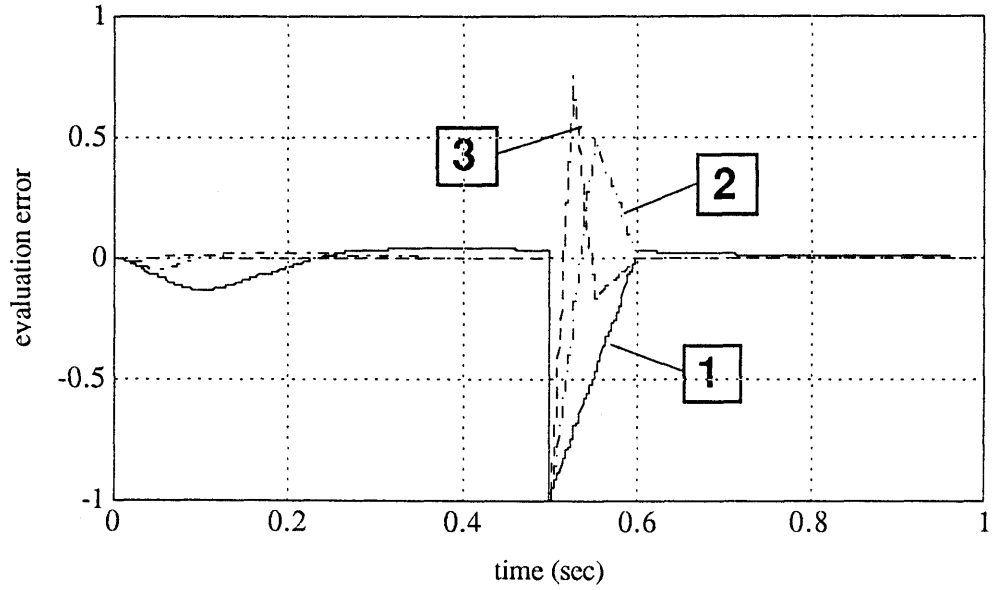

Figure 3.1: Case I: The evaluation errors of unknown function.

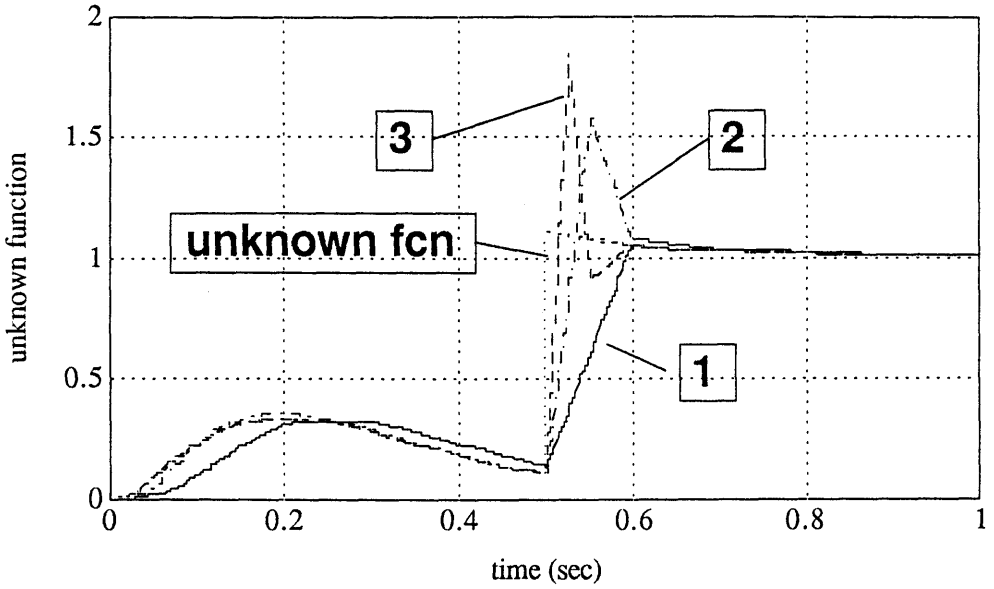

Figure 3.2: Case I: The evaluated unknown functions.

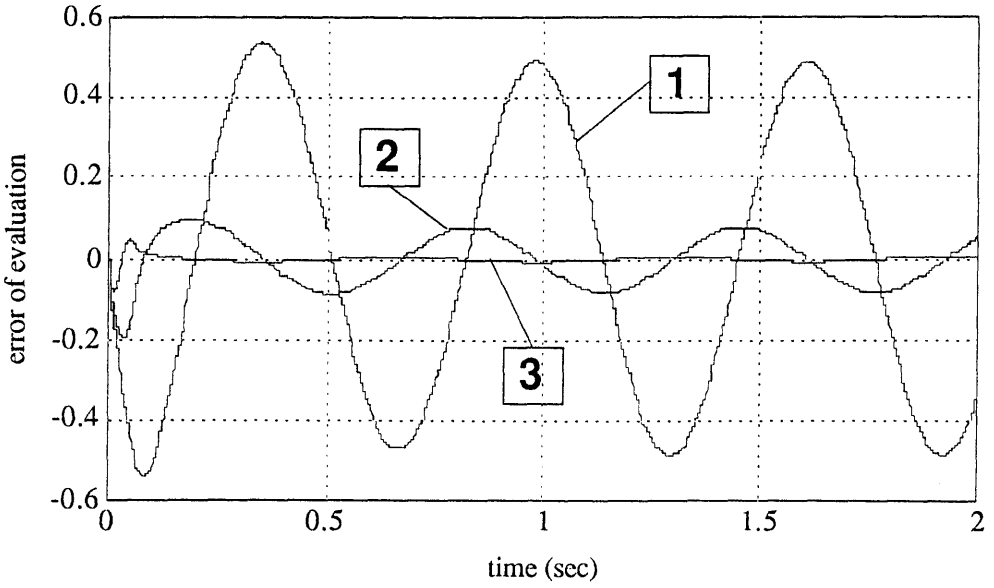

Figure 3.3: Case II: The evaluation errors of unknown function.

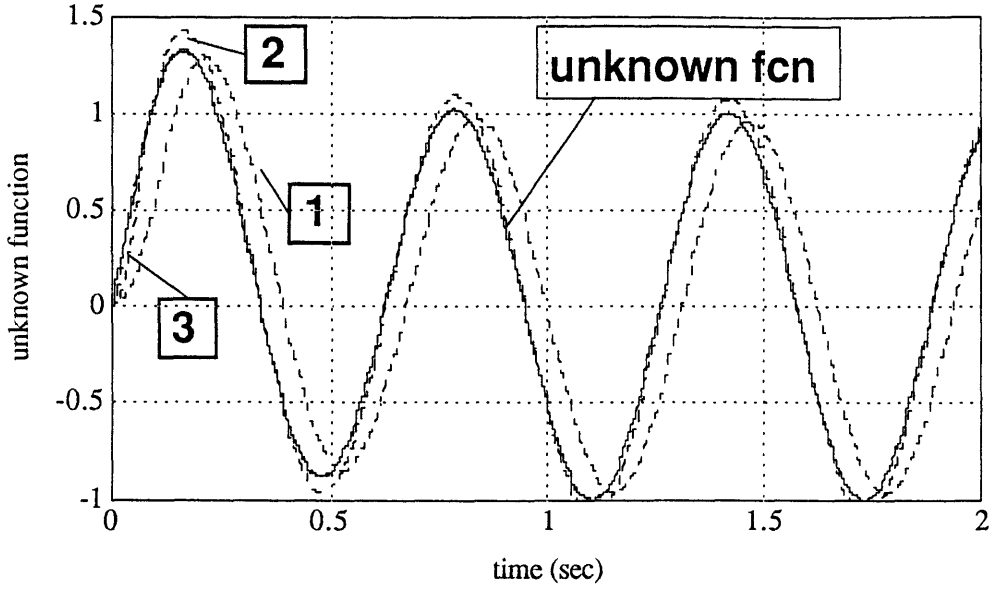

Figure 3.4: Case *II*: The evaluated unknown functions.

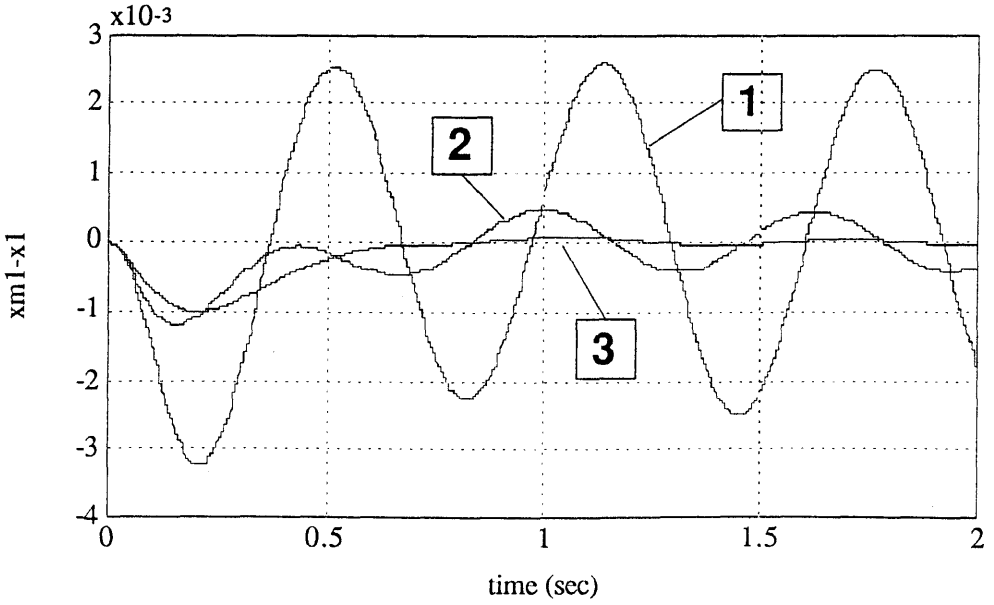

Figure 3.5: Case *II*: The tracking error of x1.

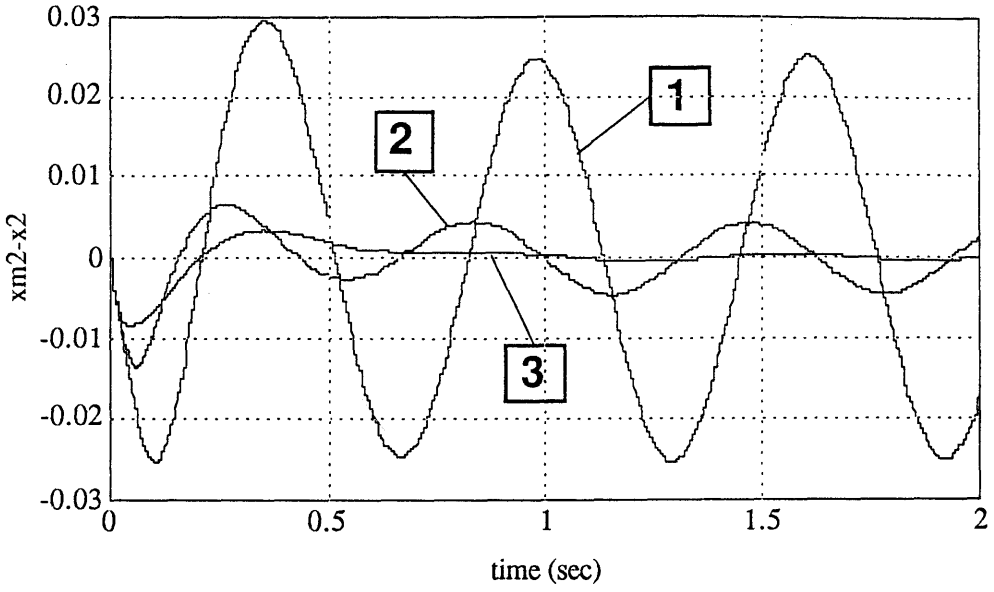

Figure 3.6: Case *II*: The tracking error of x2.

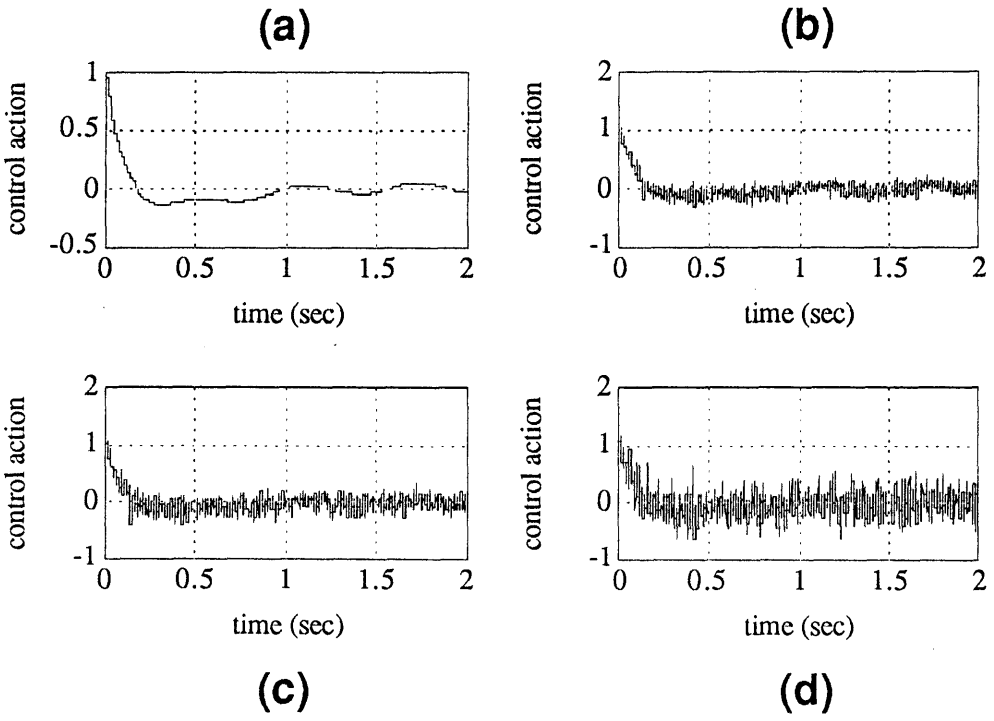

Figure 3.7: Case *II*: The control actions with 3% noise at the feedback signal. (a) no noise. (b) control action using $\hat{\Psi}$. (c) control action using $\hat{\Psi}_{order2}$. (d) control action using $\hat{\Psi}_{order3}$.

Chapter 4

The Stability Conditions

4.1 Stability Conditions for TDC Based on Convolutions

In this chapter, a method similar to reference [27] is used to discuss the stability conditions. First it is necessary to state that the values of **B**, **F**, **D**, **H** has negligible variation within the window if L is chosen small enough. This is justified by Lemma 1 in [27]:

Lemma 1: If the system under consideration and its controller are well defined by Eqn(2.1) and (2.19), (2.22) over the interval $0 \leq t \leq T$, Then $\mathbf{B}(\mathbf{x})$, $\mathbf{F}(\mathbf{x},t)$, $\mathbf{D}(t)$, $\mathbf{H}(\mathbf{x},t)$ are uniformly continuous functions of time for $0 \leq t \leq T$.

Then the following Lemma results.

Lemma 2: Consider the system described in section 2, under the digital form of Time Delay Control with the control action as Eqn(2.19) and Eqn(2.24). If

(i) The sampling period is very small : $t_s \rightarrow 0$

(ii) $\mathbf{B}, \mathbf{F}, \mathbf{H}, \mathbf{D}$ in Eqn(2.1) have small deviation within the window L

(iii) The digital system $\mathbf{z}_{(k)} = [(\mathbf{I} - \mathbf{B}(\mathbf{x})\hat{\mathbf{B}}^{+})\mathbf{C}^{-1}][\sum_{n=0}^{q-1} e^{\mathbf{A}_e(q-n)t_s}\mathbf{z}_{(k-(q-n))}]$ is exponentially stable. (where $\mathbf{C}^{-1} = [\sum_{n=0}^{q-1} e^{\mathbf{A}_e(q-n)t_s}]^{-1}$, and q is the number of data points within the window L.)

then $\dot{\mathbf{e}}_{(k)} = (\mathbf{A}_m + \hat{\mathbf{B}}\mathbf{K})\mathbf{e}_{(k)}$ can be achieved as time goes on, i.e. $k \rightarrow \infty$

Proof:

Recalling the form in section 2.4, the simplification form of Eqn(2.22) is

$$\begin{aligned}\int_{t_0}^{t}\mathbf{\Phi}(t,\tau)\mathbf{\Psi}(\tau)d\tau &= \mathbf{x}(t)-\mathbf{\Phi}(t,t_0)\mathbf{x}(t_0) \\ &+\int_{t_0}^{t}\mathbf{\Phi}(t,\tau)(\mathbf{A}_m+\hat{\mathbf{B}}\mathbf{K})\mathbf{x}(\tau)d\tau-\int_{t_0}^{t}\mathbf{\Phi}(t,\tau)\mathbf{F}(\tau)d\tau \\ &-\int_{t_0}^{t}\mathbf{\Phi}(t,\tau)\hat{\mathbf{B}}\mathbf{u}(\tau)d\tau\end{aligned} \tag{4.1}$$

If a digital controller is used and let $L = qt_s$, the evaluation of unknown function becomes

$$\begin{aligned}\hat{\mathbf{\Psi}}(t) \simeq\ & [\sum_{n=0}^{q-1}e^{\mathbf{A}_e(q-n)t_s}t_s]^{-1}[\mathbf{x}(t)-e^{\mathbf{A}_e qt_s}\mathbf{x}(t-qt_s)+\sum_{n=0}^{q-1}e^{\mathbf{A}_e(q-n)t_s}\mathbf{A}_e\mathbf{x}(t-(q-n)t_s)t_s \\ & -\sum_{n=0}^{q-1}e^{\mathbf{A}_e(q-n)t_s}\mathbf{F}(t-(q-n)t_s)t_s-\sum_{n=0}^{q-1}e^{\mathbf{A}_e(q-n)t_s}\hat{\mathbf{B}}\mathbf{u}(t-(q-n)t_s)t_s]\end{aligned} \tag{4.2}$$

where the first two of the terms between the big brackets can be written as

$$\begin{aligned}\mathbf{x}(t)-e^{\mathbf{A}_e qt_s}\mathbf{x}(t-qt_s) &= \mathbf{x}(t)-e^{\mathbf{A}_e t_s}\mathbf{x}(t-t_s)+e^{\mathbf{A}_e t_s}\mathbf{x}(t-1t_s) \\ &-\ldots+\mathbf{e}^{\mathbf{A}_e(q-1)t_s}\mathbf{x}(t-qt_s)-e^{\mathbf{A}_e qt_s}\mathbf{x}(t-qt_s)\end{aligned} \tag{4.3}$$

When $t_s \to 0$, $e^{\mathbf{A}_e t_s} \simeq \mathbf{I}+\mathbf{A}_e t_s$, and $\frac{\mathbf{x}(t)-\mathbf{x}(t-t_s)}{t_s} \simeq \dot{\mathbf{x}}(t-t_s)$, the above equation becomes

$$\sum_{n=0}^{q-1}e^{\mathbf{A}_e(q-n+1)t_s}\dot{\mathbf{x}}(t-(q-n)t_s)t_s-\sum_{n=0}^{q-1}e^{\mathbf{A}_e(q-n)t_s}\mathbf{A}_e\mathbf{x}(t-(q-n)t_s)t_s \tag{4.4}$$

Let $[\sum_{n=0}^{q-1}e^{\mathbf{A}_e(q-n)t_s}]^{-1}=\mathbf{C}^{-1}$, then

$$\begin{aligned}\hat{\mathbf{\Psi}}(t) \simeq\ & \mathbf{C}^{-1}[\sum_{n=0}^{q-1}e^{\mathbf{A}_e(q-n)t_s}\dot{\mathbf{x}}(t-(q-n)t_s)-\sum_{n=0}^{q-1}e^{\mathbf{A}_e(q-n)t_s}\mathbf{F}(t-(q-n)t_s) \\ & -\sum_{n=0}^{q-1}e^{\mathbf{A}_e(q-n)t_s}\hat{\mathbf{B}}\mathbf{u}(t-(q-n)t_s)]\end{aligned} \tag{4.5}$$

From Eqn(2.14) and Eqn(2.17) the control action is

$$\mathbf{u}=\hat{\mathbf{B}}^{+}[\mathbf{A}_m\mathbf{x}+\mathbf{B}_m\mathbf{r}-\mathbf{F}(\mathbf{x},t)-\hat{\mathbf{\Psi}}(\mathbf{x},\mathbf{u},t)]-\mathbf{K}(\mathbf{x}_m-\mathbf{x}) \tag{4.6}$$

From Eqn(2.1)

$$\begin{aligned}\dot{\mathbf{x}} &= \mathbf{F}(\mathbf{x},t)+\mathbf{H}(\mathbf{x},t)+\mathbf{D}(t)\\ &\quad +\mathbf{B}(\mathbf{x})\hat{\mathbf{B}}^{+}[\mathbf{A}_m\mathbf{x}+\mathbf{B}_m\mathbf{r}-\mathbf{F}(\mathbf{x},t)-\hat{\mathbf{\Psi}}(\mathbf{x},\mathbf{u},t)]-\mathbf{B}\mathbf{K}(\mathbf{x}_m-\mathbf{x}) \qquad (4.7)\end{aligned}$$

Substitute Eqn(4.5) into the above equation

$$\begin{aligned}\dot{\mathbf{x}} &= \mathbf{F}(\mathbf{x},t)+\mathbf{H}(\mathbf{x},t)+\mathbf{D}(t)+\mathbf{B}(\mathbf{x})\hat{\mathbf{B}}^{+}[\mathbf{A}_m\mathbf{x}+\mathbf{B}_m\mathbf{r}-\mathbf{F}(\mathbf{x},t)\\ &- \mathbf{C}^{-1}[\sum_{n=0}^{q-1} e^{\mathbf{A}_e(q-n)t_s}\dot{\mathbf{x}}(t-(q-n)t_s)-\sum_{n=0}^{q-1} e^{\mathbf{A}_e(q-n)t_s}\hat{\mathbf{B}}\mathbf{u}(t-(q-n)t_s)\\ &- \sum_{n=0}^{q-1} e^{\mathbf{A}_e(q-n)t_s}\mathbf{F}(t-(q-n)t_s)]]-\mathbf{B}\mathbf{K}(\mathbf{x}_m-\mathbf{x}) \qquad (4.8)\end{aligned}$$

Since $u = \mathbf{B}^{+}(\dot{\mathbf{x}}-\mathbf{F}-\mathbf{H}-\mathbf{D})$, when $\mathbf{B},\mathbf{F},\mathbf{H},\mathbf{D}$ has small deviation within the window with size L, and if the digital form of $\mathbf{x}(t)$ is expressed as $\mathbf{x}_{(k)}$ $(t = kt_S)$, the following equation is obtained

$$\begin{aligned}\dot{\mathbf{x}}_{(k)} &= \mathbf{B}(\mathbf{x})\hat{\mathbf{B}}^{+}[\mathbf{A}_m\mathbf{x}_{(k)}+\mathbf{B}_m\mathbf{r}_{(k)}-\mathbf{C}^{-1}\sum_{n=0}^{q-1} e^{\mathbf{A}_e(q-n)t_s}(\mathbf{I}-\hat{\mathbf{B}}\mathbf{B}(\mathbf{x})^{+})\dot{\mathbf{x}}_{(k-(q-n))}]\\ &\quad -\mathbf{B}\mathbf{K}(\mathbf{x}_{m(k)}-\mathbf{x}_{(k)}) \qquad (4.9)\end{aligned}$$

Consider the equation at step $k-1$,

$$\begin{aligned}\dot{\mathbf{x}}_{(k-1)} &= \mathbf{B}(\mathbf{x})\hat{\mathbf{B}}^{+}[\mathbf{A}_m\mathbf{x}_{(k-1)}+\mathbf{B}_m\mathbf{r}_{(k-1)}-\mathbf{C}^{-1}\sum_{n=0}^{q-1} e^{\mathbf{A}_e(q-n)t_s}(\mathbf{I}-\hat{\mathbf{B}}\mathbf{B}(\mathbf{x})^{+})\dot{\mathbf{x}}_{(k-(q-n-1))t_s}]\\ &\quad -\mathbf{B}\mathbf{K}(\mathbf{x}_{m(k-1)}-\mathbf{x}_{(k-1)}) \qquad (4.10)\end{aligned}$$

Subtract these two equations and let $y_{(i)} = \mathbf{x}_{(i)} - \mathbf{x}_{(i-1)}$, since when $t_s \to 0$, $\mathbf{x}_{(k-1)} \to \mathbf{x}_{(k)}$, $\mathbf{x}_{m(k-1)} \to \mathbf{x}_{m(k)}$, $\mathbf{r}_{(k-1)} \to \mathbf{r}_{(k)}$, the result is

$$\dot{\mathbf{y}}_{(k)} = \mathbf{B}(\mathbf{x})\hat{\mathbf{B}}^{+}[-\mathbf{C}^{-1}\sum_{n=0}^{q-1} e^{\mathbf{A}_e(q-n)t_s}(\mathbf{I}-\hat{\mathbf{B}}\mathbf{B}(\mathbf{x})^{+})\dot{\mathbf{y}}_{(k-(q-n))}] \qquad (4.11)$$

let $\mathbf{z} = (\mathbf{I}-\hat{\mathbf{B}}\mathbf{B}(\mathbf{x})^{+})\dot{\mathbf{y}}$

$$\mathbf{z}_{(k)} = [(\mathbf{I}-\mathbf{B}(\mathbf{x})\hat{\mathbf{B}}^{+})\mathbf{C}^{-1}][\sum_{n=0}^{q-1} e^{\mathbf{A}_e(q-n)t_s}\mathbf{z}_{(k-(q-n))}] \qquad (4.12)$$

If only the above system is stable, that is, $\mathbf{z}_{(k)} \rightarrow 0$, and thus $\dot{\mathbf{x}}_{(k-1)} \rightarrow \dot{\mathbf{x}}_{(k)}$. The closed loop system becomes

$$\mathbf{B}(\mathbf{x})\hat{\mathbf{B}}^{+}\dot{\mathbf{x}}_{(k)} = \mathbf{B}(\mathbf{x})\hat{\mathbf{B}}^{+}[\mathbf{A}_m\mathbf{x}_{(k)} + \mathbf{B}_m\mathbf{r}_{(k)}] - \mathbf{B}\mathbf{K}(\mathbf{x}_{m(k)} - \mathbf{x}_{(k)}) \tag{4.13}$$

Multiply $\hat{\mathbf{B}}\mathbf{B}(\mathbf{x})^{+}$ to both sides and subtract Eqn(2.4) from the above equation, we have

$$\dot{\mathbf{e}}_{(k)} = (\mathbf{A}_m + \hat{\mathbf{B}}\mathbf{K})\mathbf{e}_{(k)} \tag{4.14}$$

This completes the proof.

4.2 Stability Conditions for TDC with Extrapolations

Following the same procedure, we can derive the stability conditions for the control laws which use extrapolations to evaluate the unknown function. The conditions are similar, except that condition (iii) is revised as

- The digital system

$$\mathbf{z}_{(k)} = [(\mathbf{I} - \mathbf{B}(\mathbf{x})\hat{\mathbf{B}}^{+}) \quad][\quad 2\mathbf{C}_{\frac{1}{2}}^{-1}\sum_{n=0}^{\frac{q}{2}-1} e^{\mathbf{A}_e(q-n)t_s}\mathbf{z}_{(k-(q-n))} - \mathbf{C}^{-1}\sum_{n=0}^{q-1} e^{\mathbf{A}_e(q-n)t_s}\mathbf{z}_{(k-(q-n))}] \tag{4.15}$$

  is exponentially stable.

- The digital system

$$\mathbf{z}_{(k)} = [(\mathbf{I} - \mathbf{B}(\mathbf{x})\hat{\mathbf{B}}^{+}) \quad][\quad \frac{8}{3}\mathbf{C}_{\frac{1}{4}}^{-1}\sum_{n=0}^{\frac{q}{4}-1} e^{\mathbf{A}_e(q-n)t_s}\mathbf{z}_{(k-(q-n))} - 2\mathbf{C}_{\frac{1}{2}}^{-1}\sum_{n=0}^{\frac{q}{2}-1} e^{\mathbf{A}_e(q-n)t_s}\mathbf{z}_{(k-(q-n))}$$

$$+\frac{1}{3}\mathbf{C}^{-1}\sum_{n=0}^{q-1} e^{\mathbf{A}_e(q-n)t_s}\mathbf{z}_{(k-(q-n))}] \qquad (4.16)$$

is exponentially stable.

respectively, where $\mathbf{C}_{\frac{1}{2}} = [\sum_{n=0}^{\frac{q}{2}-1} e^{\mathbf{A}_e(q-n)t_s}]^{-1}$ and $\mathbf{C}_{\frac{1}{4}} = [\sum_{n=0}^{\frac{q}{4}-1} e^{\mathbf{A}_e(q-n)t_s}]^{-1}$.

4.3 SISO systems

4.3.1 Stabilizing Control Input Gain for TDC Based on Convolutions

When the system under considerations is a SISO system, a range for $b(x)\hat{b}^{-1}$ can be obtained. By Nyquist stability criteria, using the procedure described in [27], let $[1 - b(x)\hat{b}^{-1}]C^{-1} = \eta$, and examining the polar plot of the transfer function,

$$G(z) = \eta\frac{\sum_{n=0}^{q-1} e^{A_e(q-n)t_s}z^n}{z^q} \qquad (4.17)$$

a range $-1 \leq \eta < C^{-1}$ is found for system to be stable. Fig(4.1) and Fig(4.2) show the Nyquist plots of $G(z)$ at the two limits when $q = 12$.

4.3.2 Stabilizing Control Input Gain for TDC with Extrapolations

For the control laws which use extrapolations, the range is about $-C^{-1} < \eta \leq \alpha C^{-1}$ where α is a real number between 2 and 3. The value of α depends on q and can be obtained by Nyquist plots for each q. It is clear that the range of stable $\hat{b}^{-1}$ is reduced in the latter cases.

4.4 MIMO systems

4.4.1 Issues in MIMO Systems

For MIMO systems, the choice of the matrix $\hat{\mathbf{B}}$ that guarantees stability and acceptable performance can be difficult. Once we have $\hat{\mathbf{B}}$, the stability of the system can

be obtained by examining the equation in Lemma 2, condition (iii).

$$\mathbf{z}_{(k)} = [(\mathbf{I} - \mathbf{B}(\mathbf{x})\hat{\mathbf{B}}^{+})\mathbf{C}^{-1}][\sum_{n=0}^{q-1} e^{\mathbf{A}_e(q-n)t_s}\mathbf{z}_{(k-(q-n))}] \tag{4.18}$$

However, the choice of the elements in the matrix $\hat{\mathbf{B}}$ is not straightfoward. One way to do it is to find a stabilizing range of $\|\mathbf{I} - \mathbf{B}(\mathbf{x})\hat{\mathbf{B}}\|$, where $\|\cdot\|$ represents the norm. This leads to a more conservative result since a norm doesn't include the information about the directions in matrices. Another issue is that different norms lead to different choices of $\hat{\mathbf{B}}$. It is not clear that which definition of norm gives a better result.

4.4.2 Stabilizing Control Input Gain Matrix for TDC Based on Convolutions

Using norms, a range corresponding to a stable system is dictated by $\|\mathbf{I} - \mathbf{B}(\mathbf{x})\hat{\mathbf{B}}\|$. First, let $(\mathbf{I} - \mathbf{B}(\mathbf{x})\hat{\mathbf{B}}^{+}) = \zeta$. The stability condition Eqn (4.18) becomes

$$\mathbf{z}_{(k)} = \zeta\mathbf{C}^{-1}[e^{\mathbf{A}_e t_s}\mathbf{z}_{(k-1)} + e^{\mathbf{A}_e 2t_s}\mathbf{z}_{(k-2)} + ... + e^{\mathbf{A}_e q t_s}\mathbf{z}_{(k-q)}] \tag{4.19}$$

Taking the norms, Eqn (4.19) becomes

$$\begin{aligned}\|\mathbf{z}_{(k)}\| &\leq \|\zeta\|\|\mathbf{C}^{-1}\|[\|e^{\mathbf{A}_e t_s}\|\|\mathbf{z}_{(k-1)}\| + \|e^{\mathbf{A}_e 2t_s}\|\|\mathbf{z}_{(k-2)}\| + ... + \|e^{\mathbf{A}_e q t_s}\|\|\mathbf{z}_{(k-q)}\|] \\ &\leq \|\zeta\|\|\mathbf{C}^{-1}\|[\|e^{\mathbf{A}_e t_s}\|\|\mathbf{z}_{(k-1)}\| + \|e^{\mathbf{A}_e t_s}\|^2\|\mathbf{z}_{(k-2)}\| + ... + \|e^{\mathbf{A}_e t_s}\|^q\|\mathbf{z}_{(k-q)}\|]\end{aligned}$$

Let $\|e^{\mathbf{A}_e t_s}\| = \alpha$, $\|\mathbf{C}^{-1}\| = \beta$ and $w_{(k)} = \|\mathbf{z}_{(k)}\|$, the above equation becomes

$$w_{(k)} \leq \|\zeta\|\beta[\alpha w_{(k-1)} + \alpha^2 w_{(k-2)} + ... + \alpha^q w_{(k-q)}] \tag{4.20}$$

Since $w_{(k)} = \|\mathbf{z}_{(k)}\| \geq 0$, it is obvious that if the system described by Eqn (4.21) is stable, then Eqn (4.20) is guaranteed to be stable.

$$w_{(k)} = \|\zeta\|\beta[\alpha w_{(k-1)} + \alpha^2 w_{(k-2)} + ... + \alpha^q w_{(k-q)}] \tag{4.21}$$

Thus, the stability of Eqn (4.21) implies the stability of Eqn (4.18), since $w_{(k)} \rightarrow 0$ as $k \rightarrow \infty$ implies $\mathbf{z}_{(k)} \rightarrow \mathbf{0}$ as $k \rightarrow \infty$[1]. By the above derivation, the MIMO stability condition is reduced to a scalar system, although this is a conservative sufficient condition. The stabilizing range of $\|\zeta\|\beta$ was obtained in the previous section for SISO systems. Therefore, the stabilizing range is found to be $\|\mathbf{I} - \mathbf{B}(\mathbf{x})\hat{\mathbf{B}}\| < 1$.

4.4.3 Stabilizing Control Input Gain matrix for TDC with Extrapolations

For the control laws which use extrapolations, the range can be found by the same procedure. However, using this method, the stabilizing range is found to be the same as the cases without using extrapolations. This is because this conservative sufficient condition does not distinguish the signs of the value $[\mathbf{I}-\mathbf{B}(\mathbf{x})\hat{\mathbf{B}}]$, and only the positive part of the range is considered.

[1] Because $\|\mathbf{z}\| \rightarrow 0 \Rightarrow \mathbf{z} \rightarrow 0$

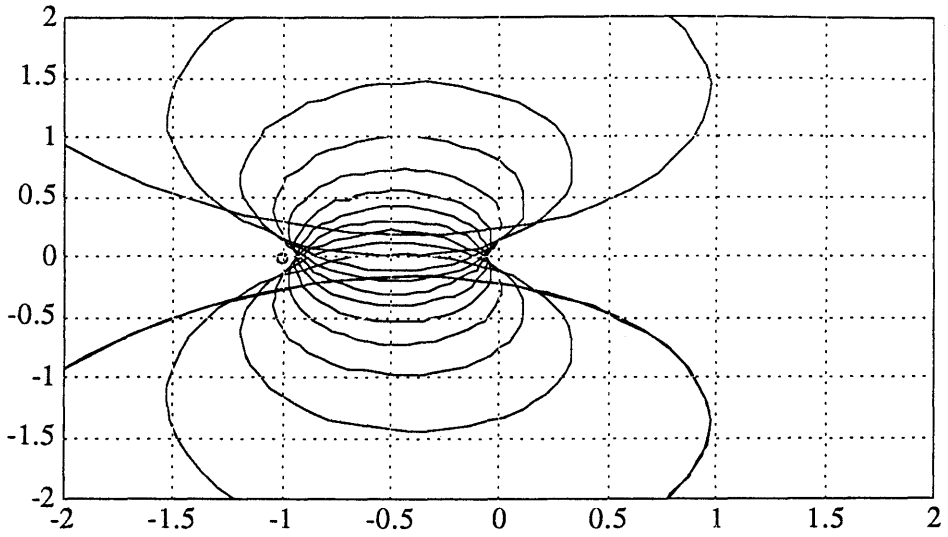

Figure 4.1: The ploar plot for $\eta = -1$.

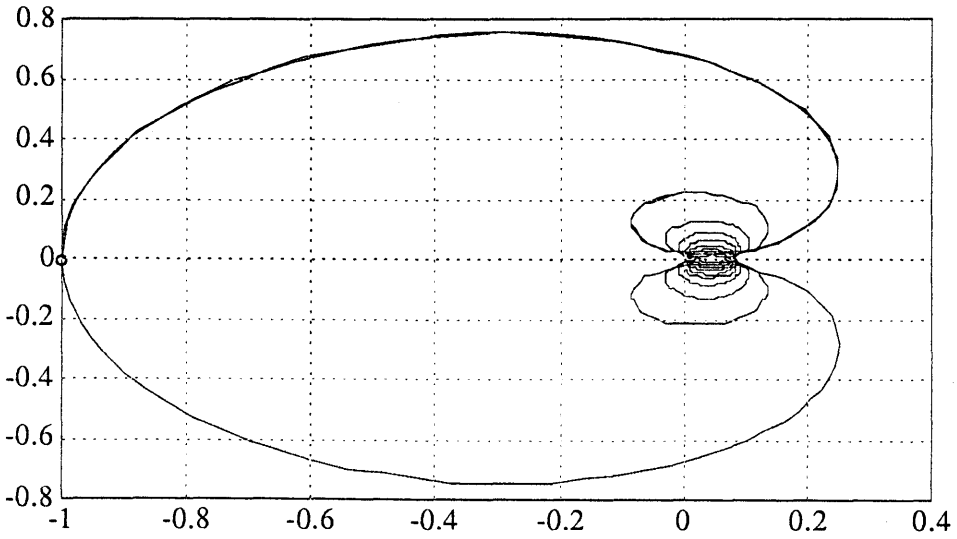

Figure 4.2: The ploar plot for $\eta = C^{-1}$.

Chapter 5

Frequency Domain Interpretation

5.1 Gain Amplification at Low Frequency

From Eqn(2.41), it is found that the estimation through digital convolutions is similar to a "Moving Average" algorithm, which is a well-known form of digital filters. However, as shown in Figure 5.1, the signals go through the moving average block include not only the feedback signals, but also the past control actions. If a linear TDC controller is considered as a special case (the case when the possibly nonlinear function $\mathbf{F}(\mathbf{x})$ doesn't appear in the control action), the whole controller fits the "Auto Regressive Moving Average Model" [9]. In this case one can examine the controller frequency response. Note that the extrapolation schemes fit the same model with different weighting coefficients. Comparing the frequency responses of the controllers using Eqn(2.24), (3.8) and (3.11), it was found that the low frequency gains are further increased by the higher order extrapolations while the high frequency response still rolls off due to the filter effects. This also gives another interpretation for the extrapolation methods that improve the command following and disturbance rejection performances while not significantly amplifying the high frequency noise.

5.2 The Effect of Digital Filter on Stability

Note that in TDC based on convolutions, the weighting coefficients are decided by the convolutions , and they are constants if $\hat{\mathbf{B}}$ is chosen as a constant matrix. If the case where the moving average only apply to feedback signals as in Figure 5.2 is considered,

then it might be possible to choose a set of weighting coefficients to reach a better filter effects in comparison to the previously mentioned controllers. Unfortunately, the system will be unstable by doing this in most of the case even when $\mathbf{B}(\mathbf{x})$ is exactly known. The reason is that the moving average algorithm introduces extra dynamics which are not counted as part of the plant. Since the relative degree is very important when designing a Time Delay Controller [26], the system is very likely to be unstable. Thus we conclude that using convolutions is a better way of introducing the filter effects while keeping the system stable with a suitably chosen $\hat{\mathbf{B}}$.

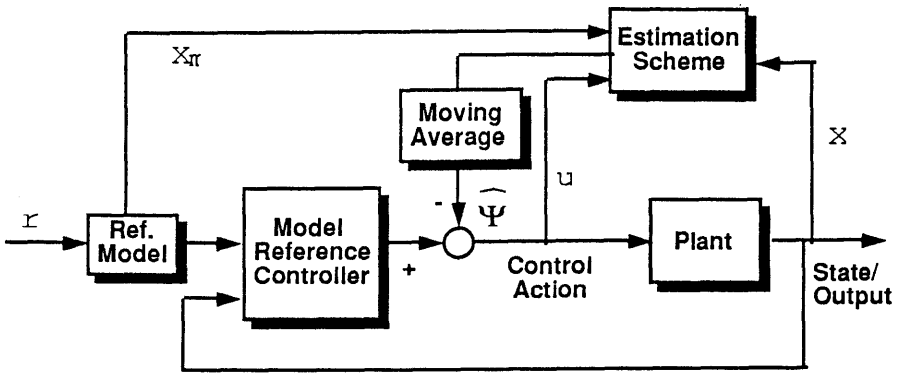

Figure 5.1: Time Delay Control schematic with moving average

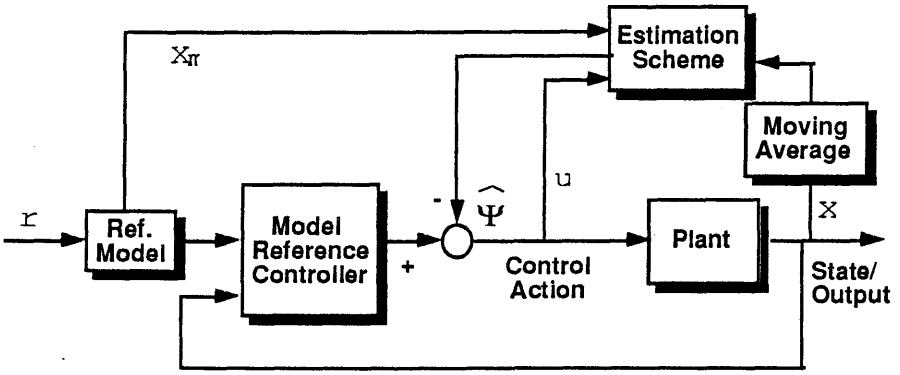

Figure 5.2: Time Delay Control schematic with moving average only on feedback signals

Chapter 6

An MIMO Example

A robot manipulator as Fig(6.1) was chosen as an example to show the effectiveness of the controllers. This system can be described by the following equations[19],

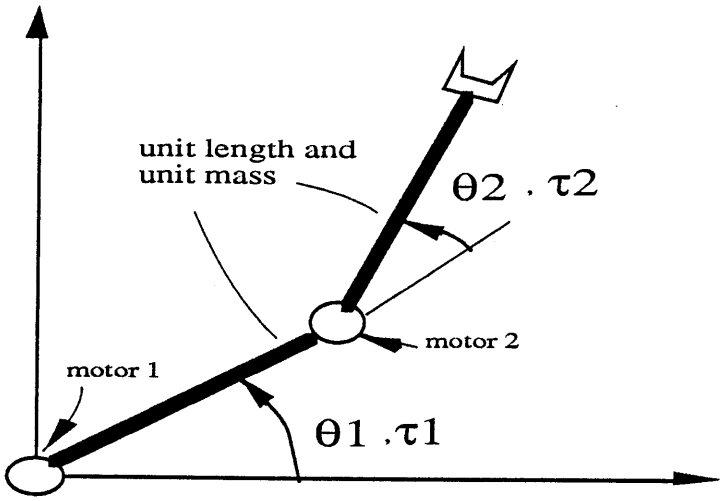

Figure 6.1: Two degree of freedom robot manipulator

$$\frac{d}{dt}\begin{bmatrix} \theta_1 \\ \theta_2 \\ -- \\ \dot{\theta}_1 \\ \dot{\theta}_2 \end{bmatrix} = \begin{bmatrix} \dot{\theta}_1 \\ \dot{\theta}_2 \\ -- \\ \mathrm{h} \end{bmatrix} + \begin{bmatrix} 0 \\ --- \\ \mathbf{H}^{-1} \end{bmatrix} \begin{bmatrix} \tau_1 \\ \\ \tau_2 \end{bmatrix} \tag{6.1}$$

where

$$\mathbf{H} = \frac{1}{2}\begin{bmatrix} 2(\frac{5}{3} + \cos\theta_2) & \frac{2}{3} + \cos\theta_2 \\ \frac{2}{3} + \cos\theta_2 & \frac{2}{3} \end{bmatrix} \tag{6.2}$$

$$\mathbf{h} = \frac{1}{2}\mathbf{H}^{-1}\begin{bmatrix} -\dot{\theta}_2(2\dot{\theta}_1 + \dot{\theta}_2)\sin\theta_2 \\ \dot{\theta}_1 \sin\theta_2 \end{bmatrix} \tag{6.3}$$

The reference model is chosen as $\xi_1 = 1, \xi_2 = 1$ and $\omega_{n1} = 5\ rad/sec, \omega_{n2} = 6\ rad/sec$ and unit step reference input for both links. The delay time is 0.1 *sec*, and the sampling period is 0.0025 *sec*. $\hat{\mathbf{B}}$ is chosen as

$$\hat{\mathbf{B}} = \begin{bmatrix} 0 & 0 \\ 0 & 0 \\ 0.75 & -0.75 \\ -0.75 & 3.75 \end{bmatrix} \tag{6.4}$$

for simulation case I and

$$\hat{\mathbf{B}} = \begin{bmatrix} 0 & 0 \\ 0 & 0 \\ 6.3750 & -15.3750 \\ -15.3750 & 40.8750 \end{bmatrix} \tag{6.5}$$

for simulation case II. Fig(6.2) to Fig(6.9) shows the results. Line 1, 2, 3 correspond to the simulation curves using $\hat{\mathbf{\Psi}}$, $\hat{\mathbf{\Psi}}_{order2}$ and $\hat{\mathbf{\Psi}}_{order3}$ respectively with the same window size $0.1sec$. Simulation results of case I show that an appropriately chosen $\hat{\mathbf{B}}$ matrix can lead to a good tracking performance, while the extrapolation scheme is used. When the $\hat{\mathbf{B}}$ matrix is poorly chosen as case II, the extrapolation scheme sometimes makes the system go unstable. Fig(6.10) to Fig(6.13) show the control actions of link 1 and link 2 when noise is added to the feedback signal. From the above, we can see that a trade-off exists among the noise effect, performance, and robustness.

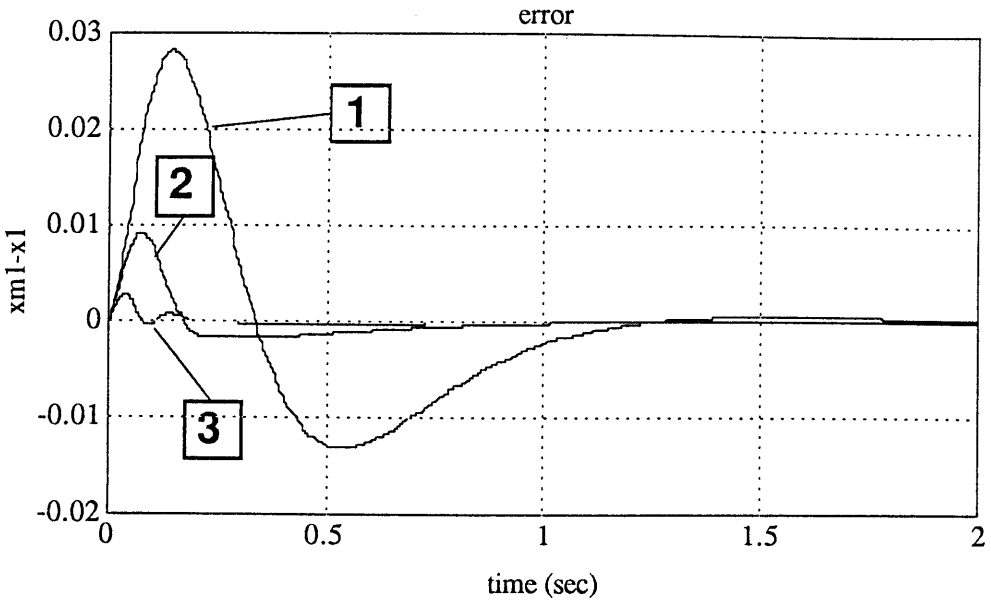

Figure 6.2: Case I: The tracking error of link1.

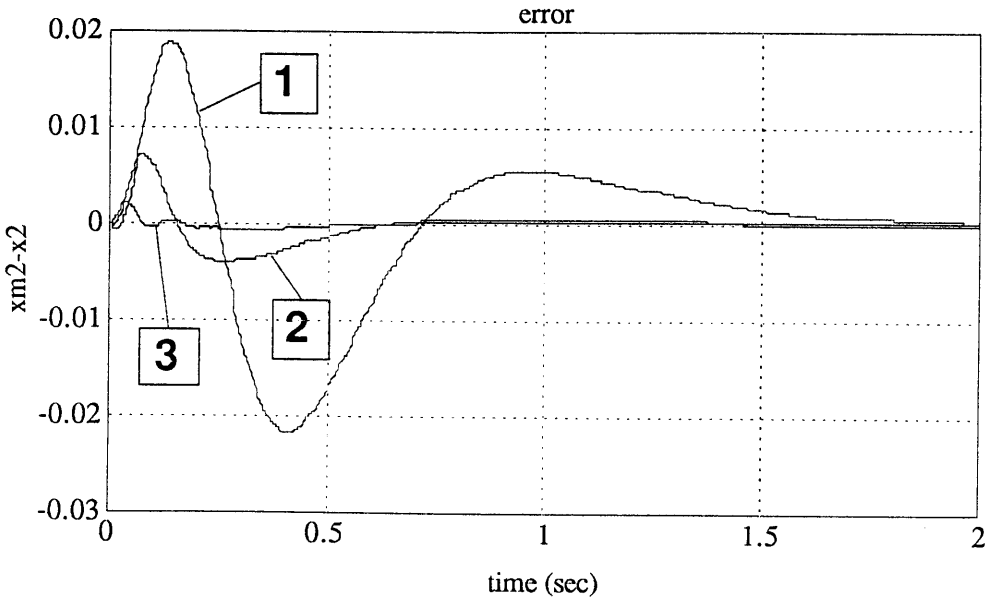

Figure 6.3: Case I: The tracking error of link2.

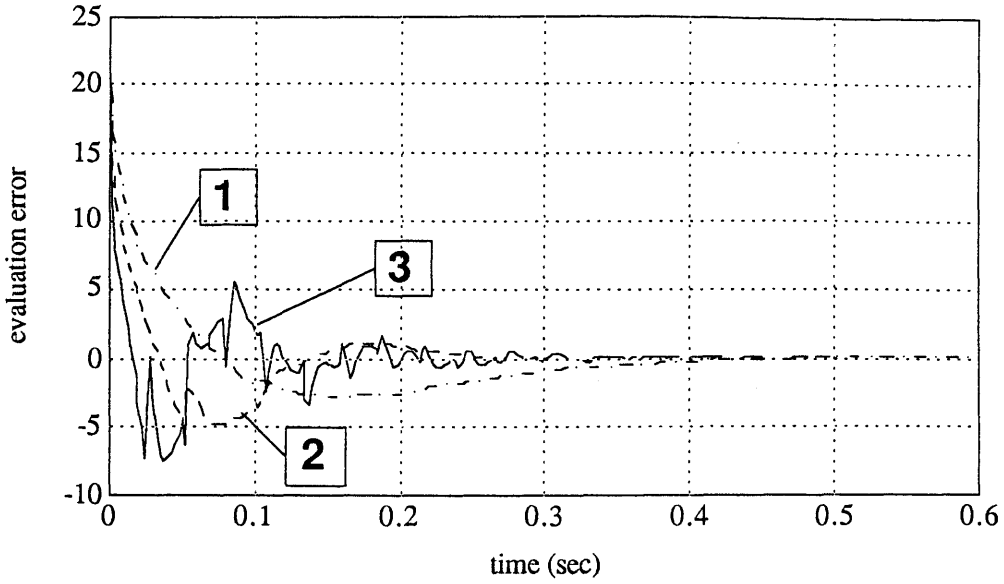

Figure 6.4: Case I: The evaluation errors of unknown function.

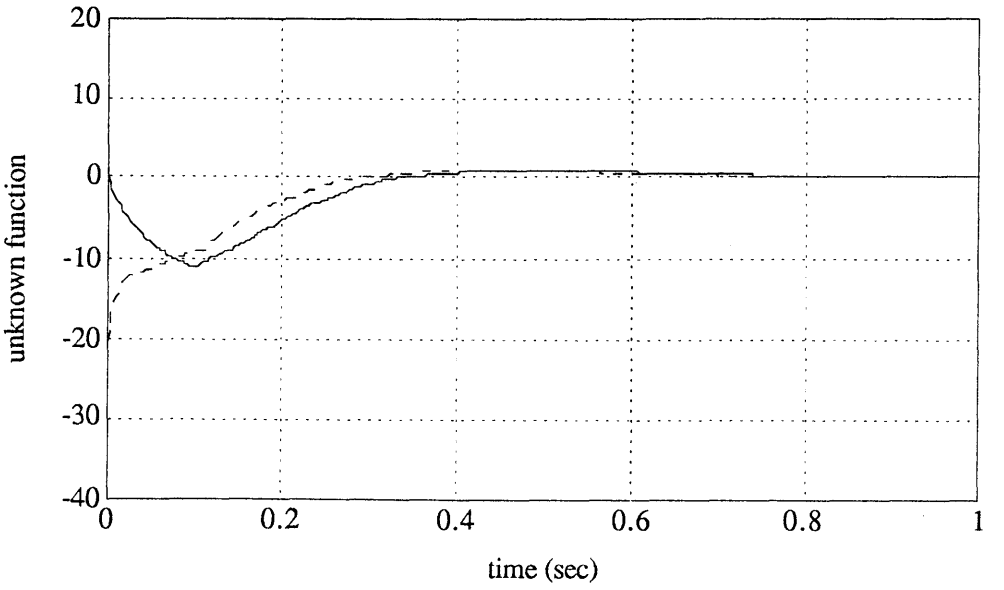

Figure 6.5: Case I: The real (- -) and evaluated (—) unknown functions by $\hat{\Psi}$.

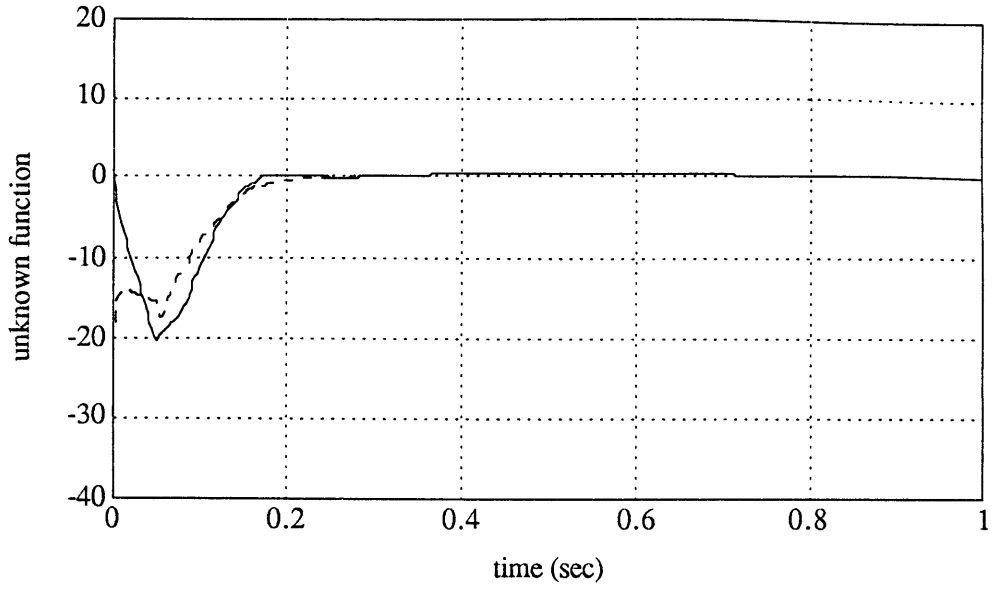

Figure 6.6: Case I: The real (- -) and evaluated (—) unknown functions by $\hat{\Psi}_{order2}$.

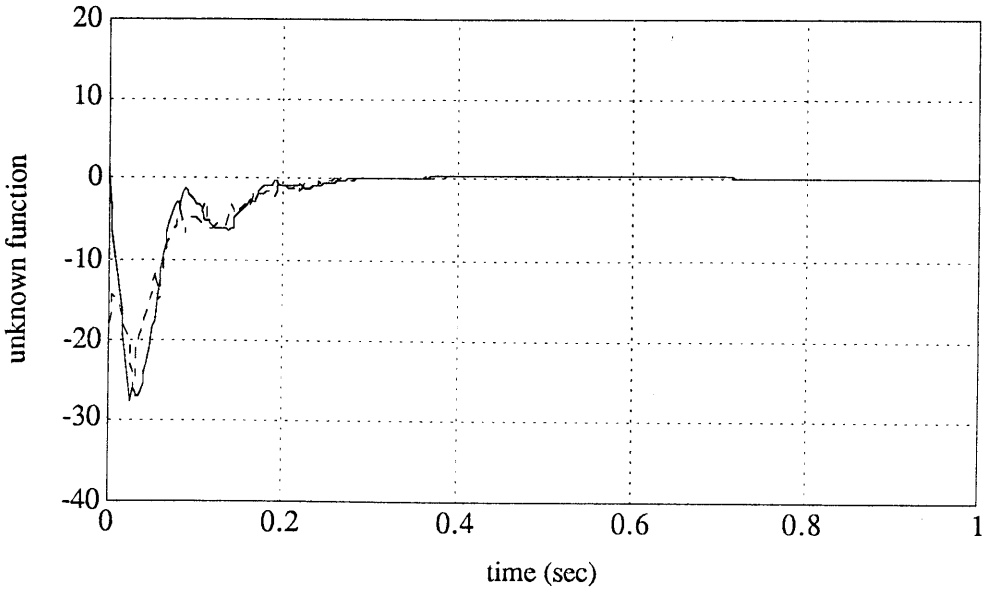

Figure 6.7: Case I: The real (- -) and evaluated (—) unknown functions by $\hat{\Psi}_{order3}$.

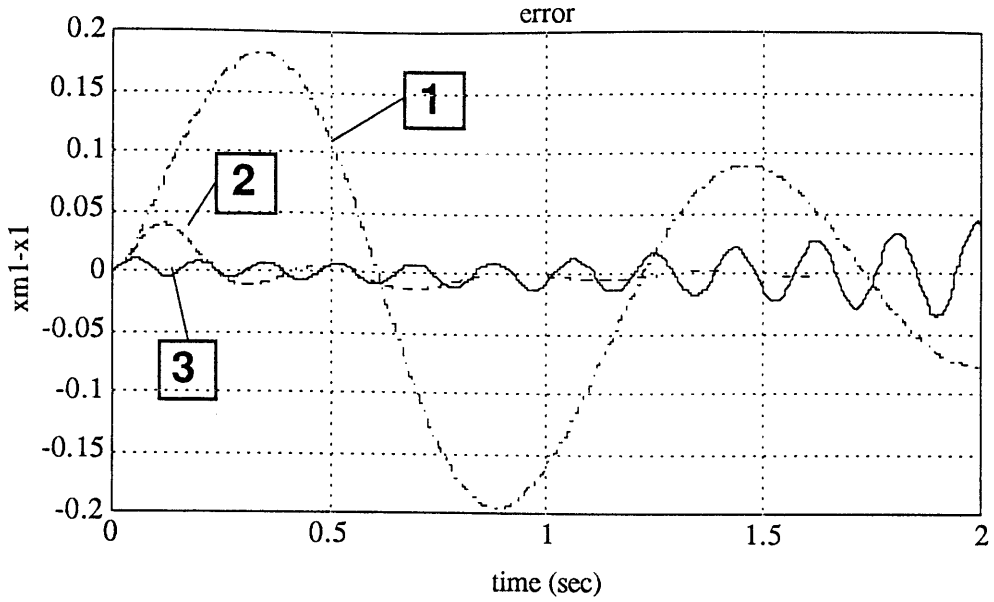

Figure 6.8: Case *II*: The tracking error of link1.

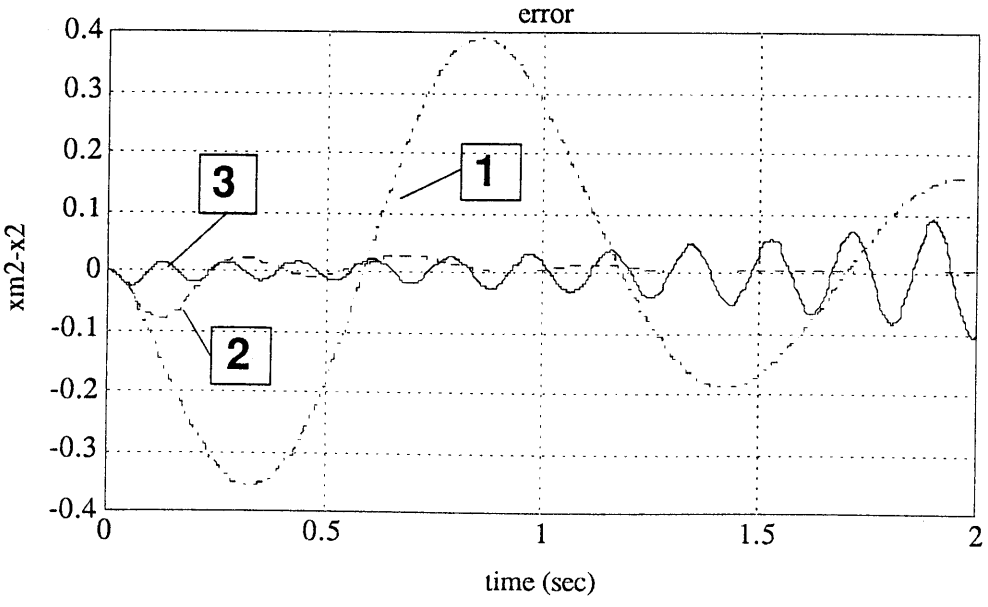

Figure 6.9: Case *II*: The tracking error of link2.

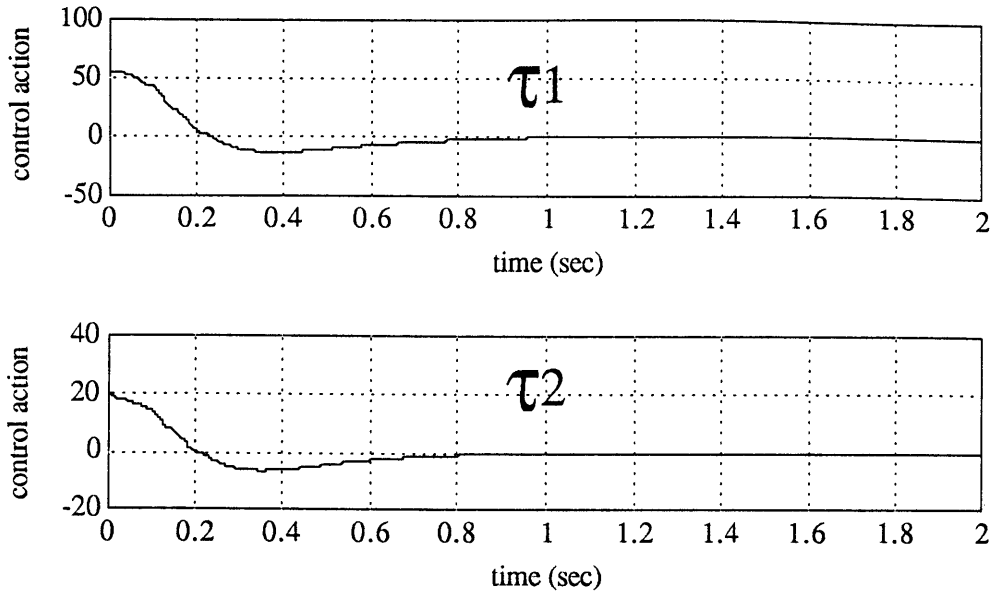

Figure 6.10: Case I: The control action by $\hat{\Psi}$.

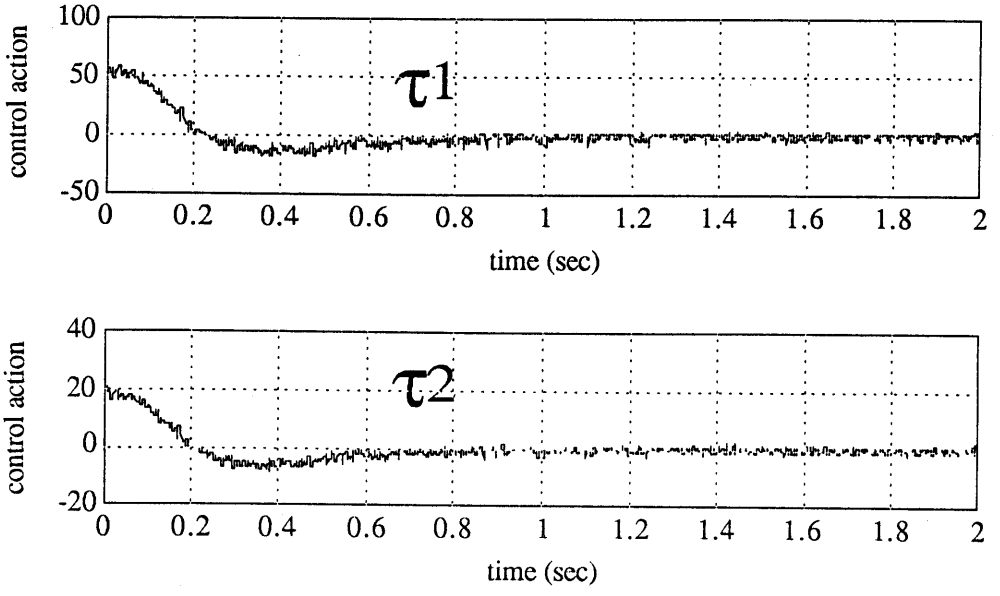

Figure 6.11: Case I: The control action by $\hat{\Psi}$ with 3% noise at feedback signal.

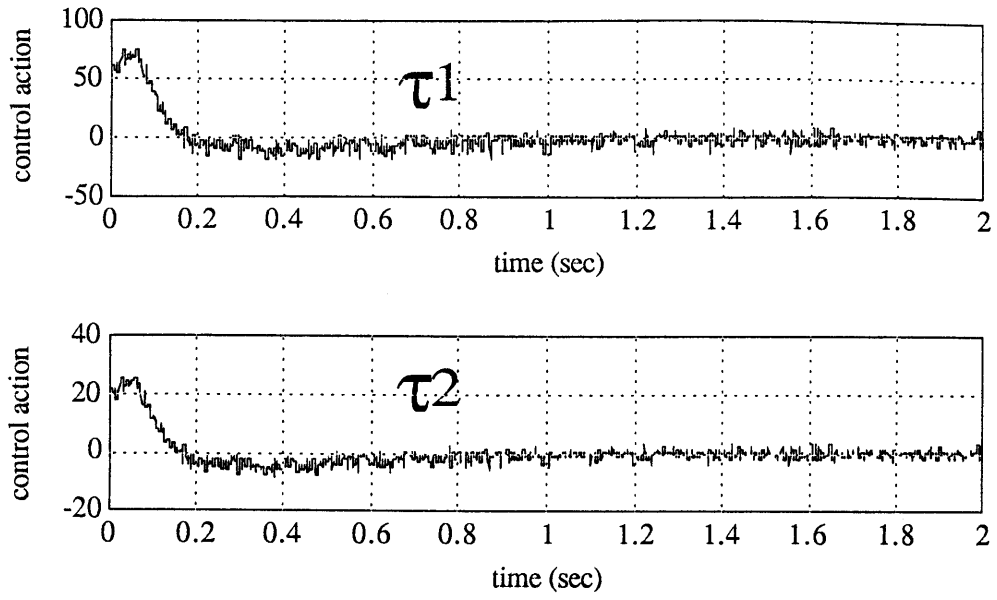

Figure 6.12: Case I: The control action by $\hat{\Psi}_{order2}$ with 3% noise at feedback signal.

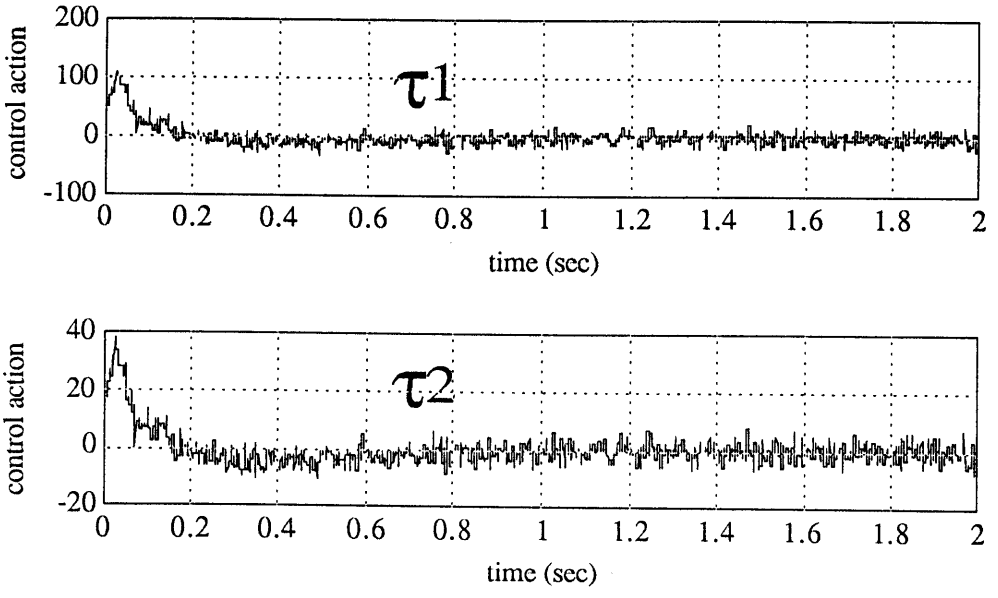

Figure 6.13: Case I: The control action by $\hat{\Psi}_{order3}$ with 3% noise at feedback signal.

Chapter 7

Application to a Cruise Control System

In this chapter, an application of Time Delay Control to an intelligent automotive cruise control system is presented to show the performance of Time Delay Control on actual systems. In this system, a vehicle is equipped with a ranging sensor which measures the distance between a preceding car and itself. The relative distance between the two vehicles is the control output [the state] of the system and the dynamics of the leading car are treated as a disturbance. The performance of the Time Delay Control Method in this intelligent longitudinal cruise control system was evaluated using a one-fifth scale car model. Through simulations and experiments, the Time Delay Control technique is shown to be well suited for intelligent cruise controls because of its rapid estimation of system dynamics changes and ease of implementation.

7.1 Introduction to an Intelligent Cruise Control System

There are several aspects to intelligent vehicle systems. For example, engine control, anti-skid braking and active suspension systems have been developed to try to automatically optimize fuel consumption, prevent wheel locking and minimize vehicle roll based on control algorithms. The driver and passengers benefits from these systems include savings, safety, and comfort.

An intelligent cruise control system may be capable of maintaining a constant speed or constant distance from a primary vehicle[1] (longitudinal control) as well as

[1]A "primary vehicle" is defined as a preceding vehicle while the "secondary vehicle", in this

directing lateral motions of the vehicle. This paper focuses on the use of Time Delay Control for longitudinal control and demonstration of its advantages. Attempting longitudinal control requires that the algorithm guarantees acceptable error dynamics (disturbance rejection) for large, unexpected disturbances. Such disturbances may be acceleration or deceleration of the primary car, changes in road conditions, changes in grade, and changes in wind. All of these disturbances will cause an error in the distance between the primary and secondary vehicles. Unless the error dynamics of the controller are guaranteed, collision avoidance could be imminent.

The control strategy considered consists of at least two levels: a high level controller and a low level controller. The high level controller may perform several functions :(1) observes the state of the system,(2) accepts inputs from environment,(3) performs filtering and estimation, (4) decides whether a task is realizable, etc.... It then generates commands which are sent to a low level controller. The low level controller on the other hand has a few other functions: (1) observes the state of the system, (2) filters and estimates and (3) computes the control action. The control action is generated in order to execute realizable commands issued by the high level controller independent of system dynamic variations. These variations may be due to internal system changes or external disturbances. Internal factors may include parameter changes and/or function changes. We are interested in designing low level controllers that guarantee the proper execution of realizable tasks.

7.2 Introduction to the System under Consideration

A one-fifth scale car model shown in Figure 7.1 is used to perform the experiment. The car model is assumed to posses a ranging sensor which could measure the distance

paper, is defined as the car intended to follow the preceding one.

between a preceding car and itself. A chassis roller was used to produce unexpected disturbances such as changes in slopes of road and inertia of the vehicle.

The system is considered as

$$\dot{\mathbf{x}} = \frac{d}{dt}\begin{bmatrix} d \\ \dot{d} \end{bmatrix} = \begin{bmatrix} \dot{d} \\ \Psi_r \end{bmatrix} + \begin{bmatrix} 0 \\ b \end{bmatrix} u \tag{7.1}$$

where d is the longitudinal relative distance (the distance between the primary car and the secondary car), Ψ_r is defined by Equation (2.7) and includes the unknown dynamics of the secondary vehicle and disturbance introduced by the primary vehicle. The reference model is defined as

$$\dot{\mathbf{x}}_m = \begin{bmatrix} \dot{d}_m \\ \ddot{d}_m \end{bmatrix} = \begin{bmatrix} 0 & 1 \\ -a_{m1} & -a_{m2} \end{bmatrix} \begin{bmatrix} d_m \\ \dot{d}_m \end{bmatrix} + \begin{bmatrix} 0 \\ b_m \end{bmatrix} r \tag{7.2}$$

The tracking error $\mathbf{e}$ between the desired relative distance trajectory d_m and the actual desired relative distance d, and the feedback gain matrix $\mathbf{K}$ are given by

$$\mathbf{e} = \begin{bmatrix} e \\ \dot{e} \end{bmatrix} = \begin{bmatrix} d_m - d \\ \dot{d}_m - \dot{d} \end{bmatrix}, \quad \mathbf{K} = \begin{bmatrix} k_1 \\ k_2 \end{bmatrix}^T \tag{7.3}$$

7.3 Controller Design

The TDC has some unique characteristics which are specially advantageous in this cruise control system. The experiments presented in this section are intended to show these effects. One of them is the tracking of a reference model which guarantee smooth acceleration and desired velocity, and position curves. The controller guarantees system robustness without detailed knowledge of the system dynamics. Consequently, the controller is easy to design and implement. Moreover, the effect of fast disturbance rejection enables the controller to use the relative distance as a feedback signal, observing the changing position of the primary vehicle as a disturbance, and reject it in several sampling periods. This can be achieved by using the

relative values as the states of the system. This effect makes the action of vehicle following possible, while other controllers may use absolute position, velocity, and acceleration signals to control the relative distance or velocity.

The control action can be calculated according to Equation (2.19) and (2.24). As a first attempt to design the controller for this system, an original TDC controller (using only one past data point) is used [2]. Since it is implemented digitally, a difference equation must be used,

$$\begin{aligned} u(k) = u(k-1) \quad &+ \quad \frac{1}{\hat{b}}[a_{m1}d(k) + a_{m2}\dot{d}(k) + \ddot{d}(k-1) + b_m r(k) \\ &+ \quad k_1 e(k) + k_2 \dot{e}(k)] \end{aligned} \tag{7.4}$$

where $\hat{b}$ is the estimate of the control input gain b. r is the reference input representing the desired relative distance which is selected as a step function. To avoid the damage of equipment, a slow response reference model is chosen ($a_{m1} = -2$ and $a_{m2} = -1$) and k_1, k_2 as error feedback gains are set to zero. These parameters can be designed based on real car limitation and desired performance. The delay time L is selected to be equal to the sampling period (8msec). Figure 7.2 shows a block diagram representation of the control law.

Note that the relative distance is the only feedback signal, which is assumed to be available in practical implementation. But, in this experiment, it is calculated by a generated signal x_p, which is selected as a ramp (i.e. the primary car is moving at constant speed) and measured signal x_s. $\dot{d}$ and $\ddot{d}$ are calculated numerically.

[2] In this case, since the feedback signal is calculated by the computer, there is no noise at the signal. Therefore, the convolution methods in previous chapters are not necessary here. If the signal is noisy, the controller need to be redesigned by the convolution methods

7.4 Experiment results

The first experiment (as Case I) involves no external disturbances imposed on the car wheels and the car starts from zero initial conditions(zero velocity and position).

Figure 7.3 to Figure 7.12 shows the simulation results and the experiment results, where x_p and x_s represent respectively the absolute position of primary and the secondary vehicle. v_p and v_s are the absolute velocities, and u_t is the control action [3]. The diagrams show that the performance is as expected despite the motion reversal which is somewhat unfeasible in a pratical situation. The settling time is about 6 sec. There is no overshoot as expected by the reference model, and the velocity curve is smooth. Also,by choosing a suitable reference model, a desired range of acceleration and jerk value can be guaranteed.

A more practical condition is then considered and the second experiment (as Case II) is performed. In this case, the system inertia is increased by having the car interact with the chassis roller. Also, in order to eliminate the motion reversal, the secondary car is kept steady until the desired distance is reached. This simple algorithm works well and does indeed eliminate the motion reversal as shown in Figure 7.13 to Figure 7.22. This case, however, is with different initial conditions. Also, the time rate of change of d is computed only after the first few samples in order to obtain meaningful data. This calculation procedure eliminates any initial jumps at the beginning of the response, which are easily seen in the previous experiment. Note that following a vehicle at any initial condition with limited time and reasonable acceleration(deceleration) sometimes is impossible, since the initial relative distance can be too large or too small in comparison with the reference input. This is true even when a reference model is introduced. Effective planning of the reference input

[3] Scale:100=1m, $\frac{1}{b} = .1176$

r(t) can possibly cope with this situation.

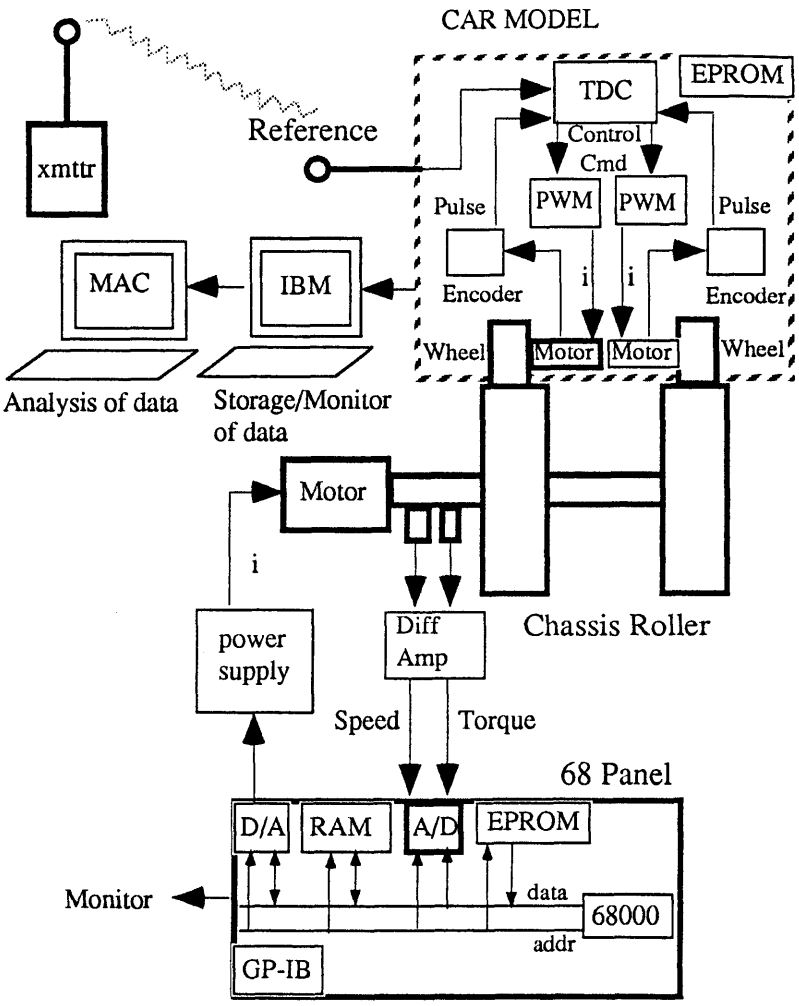

Figure 7.1: System Schematic

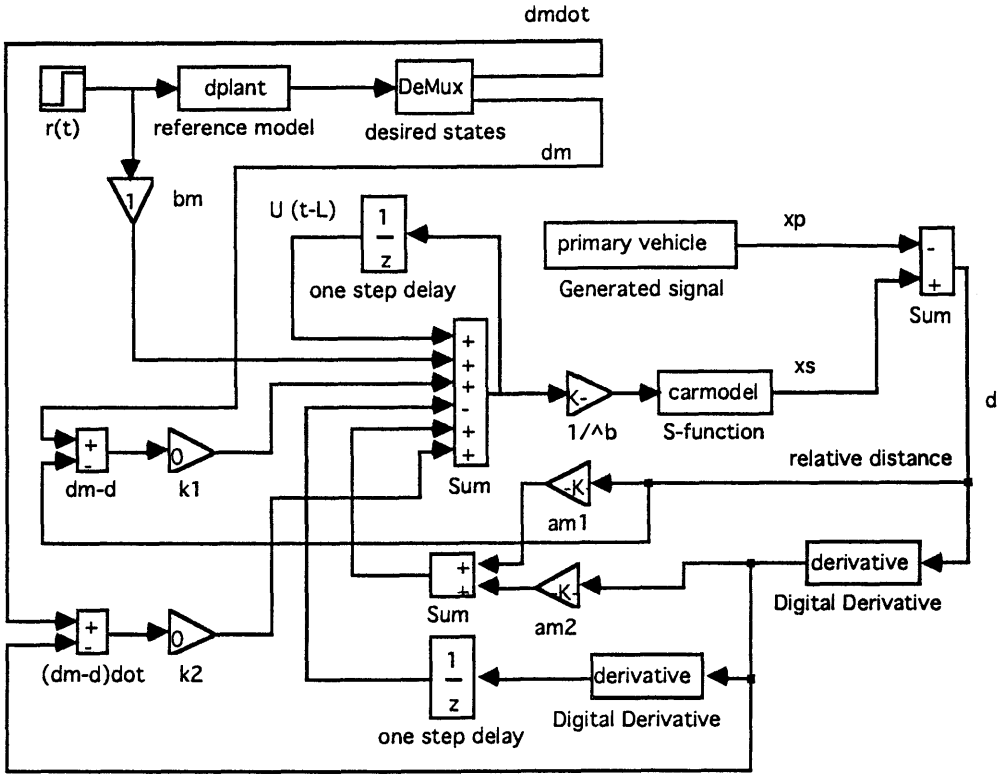

Figure 7.2: TDC controller block diagram

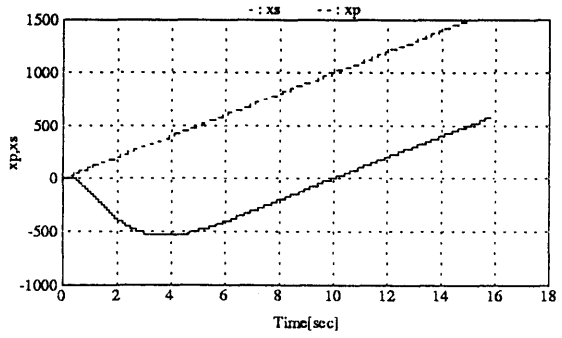

Figure 7.3: Case I : Simulation, x_p : the absolute position of primary vehicle. x_s : the absolute position the secondary vehicle.

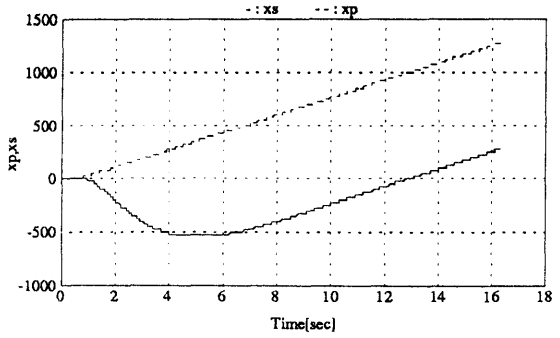

Figure 7.4: Case I : Experiment, x_p : the absolute position of primary vehicle. x_s : the absolute position the secondary vehicle.

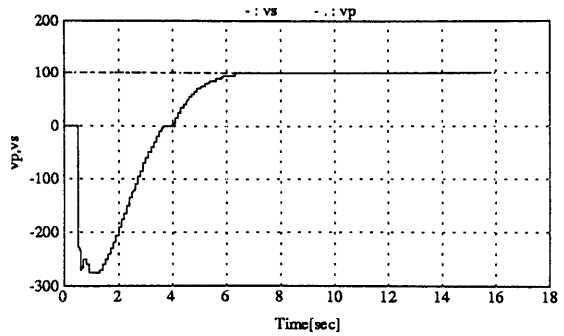

Figure 7.5: Case I : Simulation, v_p : the absolute velocity of primary vehicle. v_s : the absolute velocity the secondary vehicle.

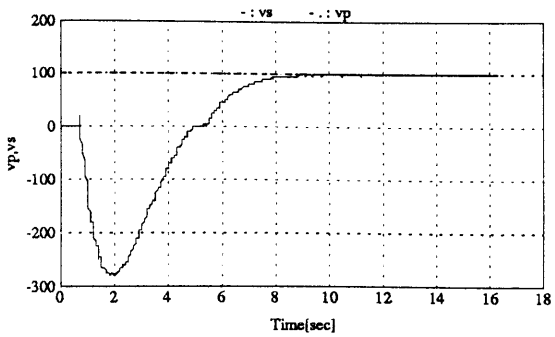

Figure 7.6: Case I : Experiment, v_p : the absolute velocity of primary vehicle. v_s : the absolute velocity the secondary vehicle.

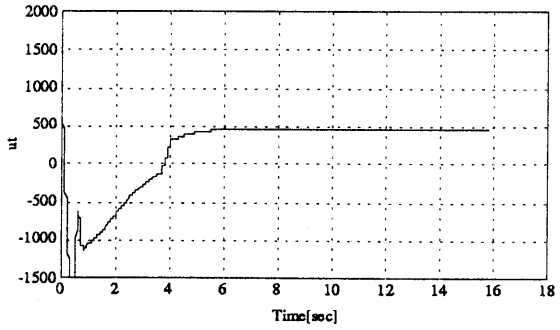

Figure 7.7: Case I : Simulation, u_t : the control action.

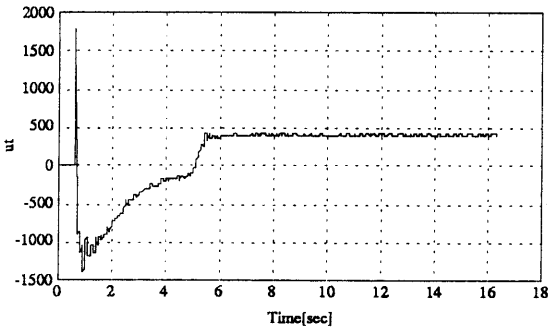

Figure 7.8: Case I : Experiment, u_t : the control action.

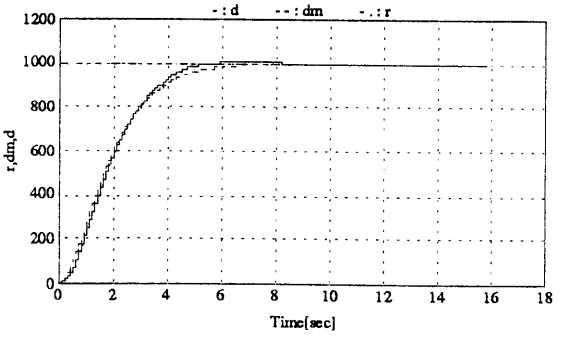

Figure 7.9: Case I : Simulation, r : the reference input. d_m : the desired relative position. d : the actual relative position.

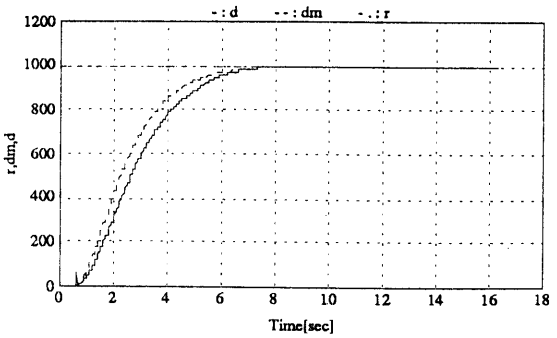

Figure 7.10: Case I : Experiment, r : the reference input. d_m : the desired relative position. d : the actual relative position.

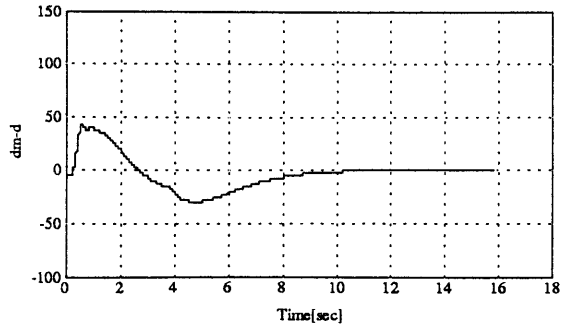

Figure 7.11: Case I : Simulation, $d_m - d$: the tracking error.

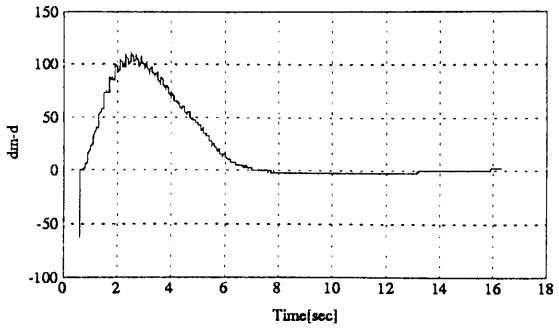

Figure 7.12: Case I : Experiment, $d_m - d$: the tracking error.

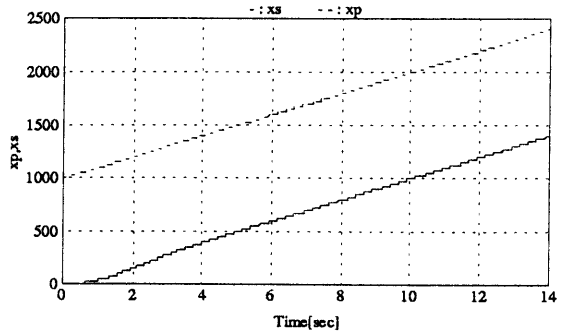

Figure 7.13: Case II : Simulation, x_p : the absolute position of primary vehicle. x_s : the absolute position the secondary vehicle.

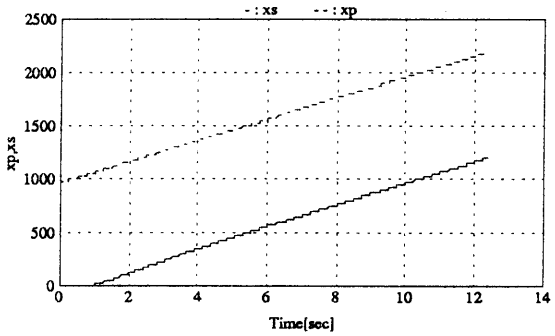

Figure 7.14: Case II : Experiment, x_p : the absolute position of primary vehicle. x_s : the absolute position the secondary vehicle.

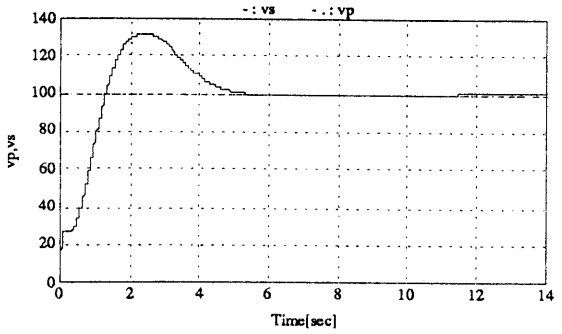

Figure 7.15: Case II : Simulation, v_p : the absolute velocity of primary vehicle. v_s : the absolute velocity the secondary vehicle.

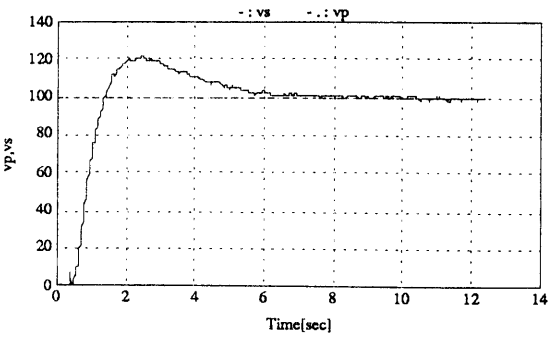

Figure 7.16: Case II : Experiment, v_p : the absolute velocity of primary vehicle. v_s : the absolute velocity the secondary vehicle.

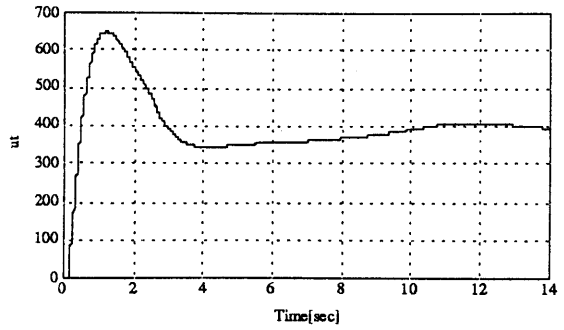

Figure 7.17: Case II : Simulation, u_t : the control action.

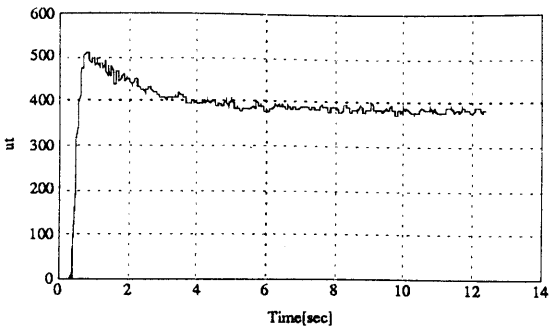

Figure 7.18: Case II : Experiment, u_t : the control action.

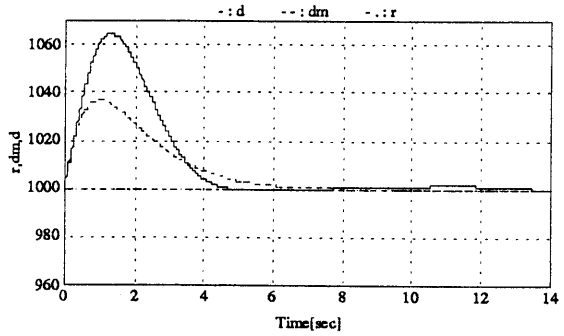

Figure 7.19: Case II : Simulation, r : the reference input. d_m : the desired relative position. d : the actual relative position.

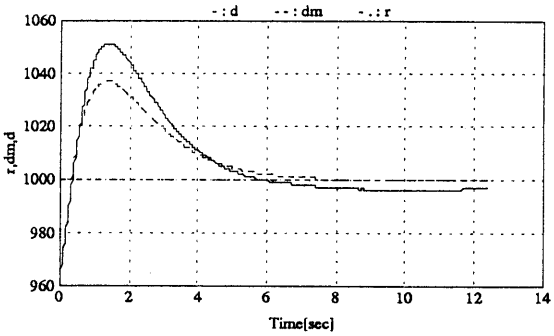

Figure 7.20: Case II : Experiment, r : the reference input. d_m : the desired relative position. d : the actual relative position.

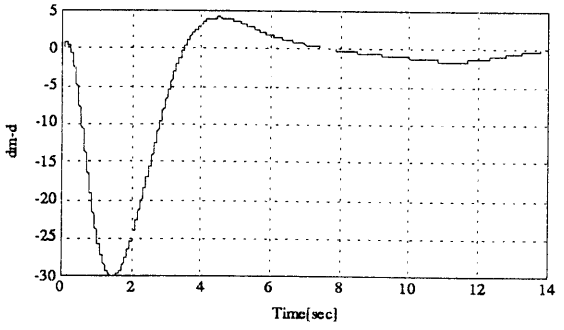

Figure 7.21: Case II : Simulation, $d_m - d$: the tracking error.

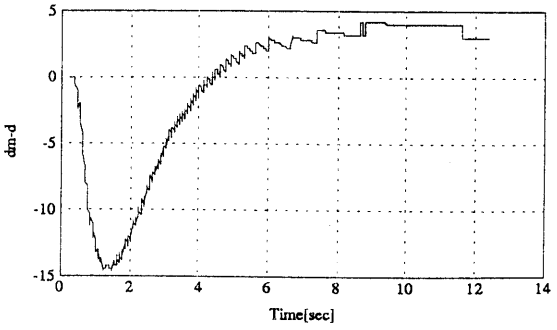

Figure 7.22: Case II : Experiment, $d_m - d$: the tracking error.

Chapter 8
Conclusion

In this thesis, the convolution type of Time Delay Control law has been derived. This control law uses a delay time larger than the sampling period to reduce the noise amplification. The accuracy of evaluation and the stability conditions are also discussed. An extrapolation method based on Taylor's expansion is suggested to improve the accuracy of the evaluation. The simulation results show that for a class of systems with unknown functions with low changing rate during the delay time, the suggested method can effectively improve the performance. The trade-off is between performance and noise amplification with reduction in the stability range.

An application of Time Delay Control (TDC) in an intelligent cruise control is also presented , under the assumption that a ranging signal is available. A car model is controlled by TDC algorithm to follow a generated position signal, which can be any reasonable function of time to simulate the primary vehicle action. The dynamics of the primary vehicle then is looked as a time varying disturbance, and TDC can reject them effectively. Simulation and experimental results demonstrate a smoothness tracking action, in both experiments under different conditions. The response time and range of acceleration can be guaranteed by choosing a suitable reference model. Some high level controller issues still need to be investigated, such as, the planning of reference input or the situation where ranging signal is not reliable. However, the successful implementation of a low level controller using TDC already affords a useful tool in the whole control structure. If noise is a significant problem, the method based on convolutions and extrapolations can be used to attenuate the

noise while keeping a good performance. This implementation and the above analysis show that the flexibility and feasibility of Time Delay Controller are largely increased by the method based on convolutions.

Bibliography

[1] Arimoto, S., Kawamura, S. and Miyazaki, F. "Can Mechanical Robots Learn by Themselves?" Proceeding of Second International Symposium on Robotics Research, Kyoto, Japan, August, 1984.

[2] Asada, H. and Slotine. Robot Control and Analysis Wiley and Sons, NY, p. 143, 1986.

[3] Astrom, K.J. and Wittenmark, B. "On Self-Tuning Regulators" Automatica, Vol. 9, pp. 185-199, 1973.

[4] Craig, J.J., Hsu, P. and Sastry, S.S. "Adaptive Control of Mechanical Manipulators", Proceeding of the IEEE International Conference on Robotic and Automation, April 7-10, 1986.

[5] Dubowsky, S. and DesForges, D.T., "The Application of Model Reference Adaptive Control to Robotic Manipulators" ASME Journal of Dynamic Systems, Measurement and Control, 101:193-200, 1979.

[6] Hsia, T.C. "Adaptive Control of Robot Manipulators - A Review" Proceeding of the IEEE International Conference on Robotics and Automation, April 7-10, 1986.

[7] Hauser, John E. "Learning Control for a Class of Nonlinear Systems", Proceedings of the 28th Conference on Decision and Control, pp.859-860, December 1987.

[8] Ih, C.C. and Wang, S. J. "Dynamic Modelling and Adaptive Control for Space Stations" JPL Publication 85-57, July, 1985.

[9] Ljuang, Lennart. *System Idetification-Theory for the User*, Prentice-Hall. 1988

[10] John R. Rice. *Numerical Methods, Software, and Analysis*, McGRAW-HILL Co. 1983

[11] Slotine, J. J.E. and Sastry, S.S. "Tracking Control of Nonlinear Systems Using Sliding Surfaces with Applications to Robot Manipulators" International Journal of Control, 38-2, 465-492, 1983.

[12] Tomizuka, M. and Horowitz, R. "Model Reference Adaptive Control of Mechanical Manipulators", IFAC Adaptive Systems in Control and Signal Processing, San Francisco, CA, 1983.

[13] Uchiyama, M. "Formulation of High-Speed Motion Pattern of a Mechanical Arm by Trial", Transaction of Society of Instrument and Control Engineering of Japan, Vol. 14, No. 6, pp. 706-712, December, 1978.

[14] Utkin, V.I. "Equations of Sliding Mode in Discontinuous Systems" Automation and Remote Control I(II), 1972.

[15] Utkin, V.I. "Variable Structure Systems with Sliding Modes", IEEE Trans. on Automatic Control, Vol. 22, pp.212-222,1977.

[16] Youcef-Toumi, K. and Ito, O. "On Model Reference Control Using Time Delay for Nonlinear Plants with Unknown Dynamics", M.I.T. Report LMP/RBT 86-06, June, 1986.

[17] Youcef-Toumi, K. and Ito, O. "Controller Design for Systems with Unknown Dynamics" Proceeding of American Control Conference, Minneapolis, MN, June, 1987.

[18] Youcef-Toumi, K. and Ito, O. "Model Reference Control Using Time Delay for Nonlinear Plants with Unknown Dynamics", Proceeding of Inter National Federation of Automatic Control World Congress, Munich, Federal Republic of Germany, July, 1987.

[19] Youcef-Toumi, K. and Ito, O. "Controller Design for Systems with Unknown Dynamics" Proceeding of American Control Conference, Atlanta, GA, June, 1988. The ASME Journal of Dynamic Systems, Measurement, and Control, Vol. 112, pp. 133-142, March 1990.

[20] Youcef-Toumi, K. and Leung, Y.F. "Analysis of Time Delay Controllers for Linear SISO Systems", Proceedings of 1988 USA-Japan Symposium on Flexible Automation.

[21] Youcef-Toumi, K. "The Control of Systems with Unknown Dynamics with Application to Robot Manipulators", M.I.T. Laboratory for Manufacturing and Productivity, Report No. 90-003, March 1990, and The ASME Winter Annual Meeting, 1990.

[22] Youcef-Toumi, K. and Reddy, S. "Stability Analysis of Time Delay Control with Application to High Speed Magnetic Bearings" M.I.T. Laboratory for Manufacturing and Productivity Report No. LMP-90-004, March 1990, and The ASME Winter Annual Meeting, 1990.

[23] Youcef-Toumi, K. and Wu, S-T "Input/Output Linearization Using Time Delay Control" M.I.T. Laboratory for Manufacturing and Productivity Report No.

LMP-90-018, September 1990. American Control Conference, June 1991. The ASME Journal of Dynamic Systems, Measurement, and Control, March 1992.

[24] Youcef-Toumi, K. "Control of Systems with Unknown Dynamics with Application to Robot Manipulators", ASME Winter Annual Meeting 1990.

[25] Youcef-Toumi, K. and Reddy, S. "Stability Analysis of Time Delay Control with Application to High Speed Magnetic Bearings", ASME Winter Annual Meeting 1990.

[26] Youcef-Toumi, K. and Wu, S-T "Input/Output Linearization Using Time delay", The ASME Journal of Dynamic systems Measurement and Control, March 1990.

[27] Youcef-Toumi, K. and Wu, S-T "Robustness and Stability Analysis of Time Delay Control", *Proceedings of the 1992 American Control Conference.*

[28] Youcef-Toumi K., Y. Sasage, J. Ardini and S.Y. Huang "The Application of Time Delay Control to an Intelligent Cruise Control System", Proceedings of the 1992 American Control Conference.